

**A novel chitosan based injectable hydrogel for  
Cartilage Tissue engineering**

**A THESIS SUBMITTED**

**BY**

**“CHINCHU K SABU”**

**IN PARTIAL FULFILLMENT OF THE REQUIREMENTS**

**FOR THE DEGREE OF**

**MASTER OF PHILOSOPHY**



**SREE CHITRA TIRUNAL INSTITUTE FOR MEDICAL SCIENCES AND  
TECHNOLOGY**

**THIRUVANANTHAPURAM – 695 012**

## **DECLARATION**

I, **CHINCHU K SABU**, hereby declare that I had personally carried out the work depicted in the thesis entitled “**A novel chitosan based injectable hydrogel for Cartilage Tissue engineering**” under the direct supervision of “**LYNDA V THOMAS, SCIENTIST D, DTERT**, Biomedical Technology Wing, Sree Chitra Tirunal Institute for Medical Sciences and Technology, Thiruvananthapuram, Kerala, India. External help sought are acknowledged.

**Signature**

**Chinchu K Sabu**

**SREE CHITRA TIRUNAL INSTITUTE FOR MEDICAL SCIENCES &  
TECHNOLOGY**

**THIRUVANANTHAPURAM – 695011, INDIA**

**(An Institute of National Importance under Govt. of India)**

**CERTIFICATE**



**This is to certify that the dissertation entitled “A novel chitosan based injectable hydrogel for Cartilage Tissue engineering” submitted by Chinchu K Sabu in partial fulfilment for the degree of Master of Philosophy Technology in Biomedical Research to be awarded by this Institute. The entire work was done by her under my supervision and guidance at DTERT, Biomedical Technology Wing, Sree Chitra Tirunal Institute for Medical Sciences and Technology (SCTIMST), Thiruvananthapuram.695012.**

**Thiruvananthapuram**

**Dr. LYNDA V. THOMAS**

**Date**

**Signature**

The Thesis Entitled

**A NOVEL CHITOSAN BASED INJECTABLE HYDROGEL FOR  
CARTILAGE TISSUE ENGINEERING**

Submitted

By

**CHINCHU K SABU**

For the degree of

**Master of Philosophy**

of

**SREE CHITRA TIRUNAL INSTITUTE FOR MEDICAL SCIENCES AND  
TECHNOLOGY**

**THIRUVANANTHAPURAM**

Evaluated and approved

by

**Name of Supervisor**

**Examiners Name**

**Signature**

**Signature**

## **ACKNOWLEDGEMENTS**

I would like to express my deepest sense of gratitude and respect to my guide Dr. Lynda V Thomas, who offered continuous advice, constant encouragement, inspiring discussions and valuable suggestions to do this work with confidence. I am grateful to Dr. Prabha D Nair (Sr. Scientist G and Head of the Department of Applied Biology) for providing me facilities to carry out my work at DTERT and for her critical evaluation of my work.

I express my sincere gratitude to Dr. Asha Kishor (Director), Dr. V Kalliyana Krishnan (Dean of Academic affairs), Dr. A.V. George (Registrar), Dr. Harikrishna Varma (Head, BMT Wing) and Dr. Santhosh Kumar B (Deputy Registrar) SCTIMST for granting me permission to work in this institute and to make use of the facilities needed during the course.

I am indebted, to Dr. Maya Nandkumar A, Dr. Manoj Komath, Dr. Francis Fernandez our course coordinators, for providing me this opportunity to be a part of the MPhil group. I am also thankful to all faculty members who have painstakingly delivered excellent classes for our M.Phil course work.

My special thanks to Dr Harikrishna Bhatt, U S Hareesh, National Institute for Interdisciplinary Science and Technology (NIIST) for allowing me to use the NMR and Rheology facility at their Institute.

On personal note, I would like to thank every member of DTERT for their support and encouragement. I would like to thank Dr. Babitha, Mr. Rahul, Mrs. Neelima, Dr. Amritha, Ms. Jijo, Mrs. Nimi, Dr. Siva Das, Mr. Dhanesh, Dr. Lekshmi, Dr. Santhi, Mrs. Priyadarsini for their friendly support and helping hands.

With great pleasure, I record the encouragement, support and prayers received from my parents and sister for always being my side, for their love, sacrifices and continued encouragement throughout my life.

Last, but not the least, I thank the Almighty for the wisdom and perseverance that he has bestowed upon me during this research project, and indeed throughout my life.

Chinchu K. Sabu

# CONTENTS

ACKNOWLEDGEMENTS

LIST OF FIGURES

LIST OF TABLES

ABBREVIATIONS

SYNOPSIS

<b>DECLARATION.....</b>	<b>2</b>
<b>BACKGROUND .....</b>	<b>5</b>
1.2 Composition of articular cartilage .....	7
1.2.1 Chondrocytes .....	8
1.2.2 Extracellular matrix (ECM) .....	8
1.3 Mechanical properties of articular cartilage .....	9
1.4 Articular cartilage injuries .....	9
1.5 Surgical treatment of articular cartilage damages.....	10
1.6 Limitations of current surgical methods for cartilage repair .....	11
1.7 The concept of ‘TISSUE ENGINEERING’ .....	12
1.8 Tissue engineering of cartilage- an upcoming treatment modality.....	14
1.9 Natural polymers for cartilage regeneration .....	15
1.10 Synthetic polymers.....	16
1.11 Hydrogels.....	17
1.12 3D printing for creating cartilage constructs .....	18
1.13 Polysaccharide-based hydrogels .....	19
1.13.1 Chitosan in cartilage regeneration .....	21
1.13.2 Xanthan gum in cartilage tissue engineering .....	23
1.14 HYPOTHESIS .....	24
1.15 OBJECTIVES .....	24
1.16 SIGNIFICANCE OF THE STUDY.....	24
<b>CHAPTER 2 .....</b>	<b>25</b>
<b>MATERIALS AND METHODS .....</b>	<b>25</b>
2. MATERIALS.....	25
2.1 Preparation of xanthan gum dialdehyde .....	25
2.1.1 Determination of degree of oxidation .....	25
2.1.2 Nuclear Magnetic Resonance spectroscopy.....	26
2.2 Preparation of chitosan- xanthan gum dialdehyde (ch-xda) hydrogels .....	26
2.3 Characterization of the chitosan-xanthan gum dialdehyde based hydrogel.....	27
2.3.1 FT-IR analysis.....	27
2.3.2 Percentage degree of crosslinking .....	27

2.3.3 Gelling time determination of chitosan-xanthan gum dialdehyde gel .....	28
2.3.4 Percentage gel fraction.....	28
2.3.5 Degree of swelling .....	28
2.3.6 Rheological studies .....	29
2.4 Cytotoxicity analysis using L929 cells .....	29
2.4.1 Direct contact test .....	29
2.4.2 Test on extract (MTT assay) .....	29
2.5 Isolation of chondrocytes from rabbit articular cartilage.....	30
2.6 Encapsulation of chondrocyte in CH-XDA hydrogels .....	30
2.7 Live dead staining .....	30
2.8 Quantification of total glycosaminoglycan content .....	31
2.9 Safranin o staining and Toluidine blue staining .....	31
2.10 Immunofluorescence analysis .....	31
2.11 3D printing using the chitosan xanthan gum dialdehyde as ink .....	32

**CHAPTER 3 .....**33

**RESULTS AND DISCUSSION .....**33

3.1.Characterization of chitosan-xanthan gum dialdehyde (CH-XDA) hydrogels.....	33
3.2Biological evaluation of the chitosan-xanthan gum dialdehyde hydrogel.....	43
3.3 Chondrocyte encapsulation CH-XDA gel system.....	45

**CHAPTER 4.....**51

**CONCLUSION .....**51

**FUTURE PERSPECTIVES.....**51

## LIST OF FIGURES

Figure 1: Schematic cross sectional diagram of healthy articular cartilage.....	7.
Figure 2: Tissue engineering triad of cells, signals and the scaffold which acts as a template for tissue formation by allowing cells to migrate, adhere, and create tissue.....	12.
Figure 3: Schematic representation of methods of cartilage tissue engineering.....	14.
Figure 4: Molecular structures of the polysaccharide repeating units.....	21.
Figure 5: Chemical structures of A) chitosan and B) xanthan gum.....	23.
Figure 6: Schematic representation of the formation of CH-XDA gels through Schiff's base reaction between free amine groups on chitosan and aldehyde groups on xanthan gum dialdehyde.....	34.
Figure 7 : <sup>1</sup> H NMR spectrum showing a) xanthan gum and b) xanthan gum dialdehyde.....	36.
Figure 8 : FTIR plot of a) xanthan gum and b) xanthan gum dialdehyde.....	38.
Figure 9 : FTIR plot showing a) chitosan b) xanthan gum c) 70CH-30XDA d) 75CH-25XDA ,e) 80CH:20XDA.....	40.
Figure 11: a) Degree of swelling of three different ratios for a period of 48 hr. b) % Degree of crosslinking.....	41.
Figure 12: Rheological properties of CH-XDA hydrogel prepared in three different ratios.....	43.
Figure 13: microscopic images of Direct contact assay. A) Control B) 70CH:30 XDA C) 80CH:20XDA and D) 75CH:25XDA after 48 hr.....	44.
Figure 14: Assessment of mitochondrial activity by MTT assay.....	45
Figure 15: Cells isolated of rabbit articular cartilage a) from explants b) after digestion.....	46 .

Figure 16: Live Dead assay of encapsulated chondrocyte on 7, 14 and 21 days of culture in CH-XDA gel.....	46.
Figure 17 : a) Safranin O staining of control without cells b) safranin O staining of 21 day construct, which stains proteoglycans in the ECM c) Toluidine blue staining of control without cells d) Toluidine blue staining of 21 day scaffold construct to stain the proteoglycans and GAG.....	47.
Figure 18: a) Quantification of total GAG content by DMMB assay for 7, 14 and 21 day culture.b) immunofluorescence staining 21 day construct on collagen type II antibody.....	48.
Figure 19 : The 3D printed gel composition of 90CH:10XDA.....	49.

## **List of tables**

Table 1: Composition chart of hydrogels prepared.....	27.
Table 2: Test for chitosan (Sigma Aldrich, Cat No. 3646).....	35.
Table 3: Spectroscopic data ( <sup>1</sup> H NMR) of oxidized xanthan gum in D2O.....	37.
Table 4: Parameters standardised for 3D printing.....	49.

## List of abbreviation

SLS	Selective laser sintering
3D	3 Dimensional
BMP	Bone morphogenetic protein
DMEM-HG	Dulbecco's Modified Essential Medium –High glucose
DMMB	Dimethylmethylene blue
DMSO	Dimethyl Sulfoxide
ECM	Extracellular matrix
FBS	Fetal Bovine Serum
FDM	Fused deposition modelling
FT-IR	Fourier Transform Infrared Spectroscopy
GAG	Glycosaminoglycan
HA	Hyaluronic acid
IGF	Insulin like growth factor
NaOH	Sodium hydroxide
NMR	Nuclear Magnetic Resonance
RP	Rapid prototyping
SFF	Solid free-form technology
SLS	Selective laser sintering
TGF- $\beta$	Transforming growth factor b
TIJ	Thermal inkjet printing
XG	Xanthan Gum
XDA	Xanthan gum dialdehyde

## Synopsis

Diseases such as osteoarthritis, trauma associated with injury, chondrosarcoma and other congenital diseases form a defective cartilage where the complex metabolic balance of the cartilage is disrupted mainly due to lack of blood vessels, nerves, and lymphatics, leading to the loss in integrity of tissue and biomechanical function. According to the World Health Organization, the frequency of a damaged joint is going to increase considerably in the coming years. The currently available treatment options provide only short term relief with poor tissue regeneration. Tissue engineering is an evolving alternative treatment using autologous cells that are isolated from patient, expanded and cultured in vitro in three dimensional (3D) scaffolds which can be implanted back into the patient. Appropriate combination of 3D polymeric scaffolds, cells and signalling molecules are required for successful in vitro regeneration of the tissue.

Articular cartilage has four zones, first is the superficial zone. It helps to resist shear stresses, secretes lubricating proteins and has low fluid permeability. Next to the superficial zone is the transitional zone, the area of transition between shearing and compression forces. The third zone plays a role in load bearing distribution and resistance to compression forces. Next calcified zone is a transitional zone between hyaline cartilage and subchondral bone. This layer contains hypertrophic chondrocytes in a cartilaginous matrix. Calcified zone mainly couples the mechanical properties of bone and cartilage and this zone plays major role in maintaining structural integrity of articular cartilage. Conventional treatment strategies are not satisfactory to regenerate a potential functional cartilage.

Tissue engineering of cartilage generally utilizes a natural or synthetic matrix to serve as a 3D template for growing cells. 3D culture in culture in scaffold gives more information compared to the two dimensional cultures. 3D culture in scaffolds provides more surface area which promotes high cell-cell and cell-matrix interaction and is a better representation of actual tissue. The overall morphology of the 3D scaffolds, inbuilt properties of the materials and chemical composition may directly or indirectly influence the behavior of cells cultured on the scaffold.

This thesis has been divided into three chapters; the first chapter briefly discusses the structure, function and composition of articular cartilage. The current available status on articular cartilage diseases and treatment options and their limitation are discussed in detail. The concept and role of the three major components of tissue engineering namely, 3D scaffolds, cells and signalling molecules are discussed focusing on to chondrocyte culture in 3 D scaffolds. A literature review of the hydrogels and the emerging new technique 3 D printing techniques and its importance in manufacturing tissue engineering constructs are given. Hence the necessity to find a hybrid scaffold with better properties is pointed out and the importance of natural polymer based system for cartilage regeneration are discussed in this section.

The second chapter deals with the materials and methodology employed in the study, including fabrication of three different combinations of Chitosan-Xanthan gum dialdehyde scaffolds and chondrocyte encapsulation within the system. The novel scaffolds are characterized for its physicochemical properties and invitro cytotoxicity. The physicochemical properties of the novel hybrid materials are evaluated using techniques like, Fourier transform IR spectroscopy (FTIR), NMR and Rheology measurements. The suitability of our hydrogel to serve as a scaffold is further confirmed by analyses of its swelling, crosslinking, gelation properties. Further in this chapter the isolation and in vitro culture of rabbit chondrocytes and the culture of chondrocyte in the hybrid scaffold for a period of 7, 14 and 21 days and the compatibility of scaffold for chondrocyte culture is analysed. The cultured constructs are evaluated by biochemical assays and staining protocols.

Third chapter describes the results and discussion of the study. 70% Chitosan and 30% xanthan concentration chosen as working concentration based on the physicochemical characteristics. Chondrocyte encapsulation studies are done in this concentration to see the viability of cells in the hydrogel scaffold. The overall cell distribution, cell morphology and the production of cartilage specific matrix molecules are analysed using various biochemical and histological techniques. Thus the suitability of these scaffolds for cartilage tissue engineering is analysed.

Fourth chapter concludes that natural polysaccharide based chitosan xanthan gum hydrogels are promising scaffolds for cartilage tissue engineering applications. Future aspects of the investigation are also proposed.

# CHAPTER 1

## 1. Introduction

### Background

Articular cartilage is the highly specialized connective tissue, with 2 to 4 mm thickness providing a smooth, lubricated surface for articulation and also to facilitate the transmission of loads with a low frictional coefficient. It can support one to 9.36 MPa of force an average of two million times each year (Silva et al, 2002; Yoshida et al, 2006). As cartilage deteriorates, bones of joint begin to collide each other causing stiffness and pain further affects the movement. Articular cartilage injury can be chondral or osteochondral. Articular cartilage defects are caused mainly by trauma, joint misalignment. Articular cartilage defects are not life threatening but it can cause lifelong debilitation. The progressive degradation and destruction of articular cartilage resulting in sclerosis of subchondral bone is characterized as Osteoarthritis. Osteoarthritis is one of the most chronic health conditions and the 11th highest contributor to disability. Osteoarthritis is the most common form of arthritis can damage any joint in the body, most commonly affects joints in your hands, knees, hips and spine. It is the second most common rheumatologic problem and it is the most frequent joint disease with a prevalence of 22% to 39% in India. Osteoarthritis is more common in women than men, but the prevalence increases dramatically with age. Overall prevalence of knee osteoarthritis in India was found to be 28.7%. The associated factors were found to be female gender (prevalence of 31.6%) ( $P = 0.007$ ), obesity ( $P = 0.04$ ), age ( $P = 0.001$ ) and sedentary work ( $P = 0.001$ ). (Chandra Prakash Pal, Indian J Orthop. 2016).

Articular cartilage is devoid of blood vessels, nerves and lymphatics and so because has a limited capacity for intrinsic healing and repair. Treatments for osteoarthritis are available only to manage symptoms like pain and inflammation. Tissue engineering is one of the biomedical forms to build up the environment to induce cell based tissue

regeneration by a combination of cells, scaffolds and biological substitutes which can rebuild the structure and function of native tissue.

## **Review of literature**

Three types of cartilage exist in the human body: hyaline cartilage (e.g., within trachea, nose), fibro cartilage (e.g., intervertebral discs, joint capsules), and elastic cartilage (e.g., external ear, epiglottis). Articular cartilage is specialized hyaline cartilage that covers the bone surfaces exhibits superior lubrication, wear, and low friction properties. It is composed of two phases – solid and liquid. The interactions between these two phases characterize the viscoelastic properties of this tissue. In this, 60–80% of total wet weight is fluid which contributes many important physical and physiological characteristics of articular cartilage. The remaining 20–40% of the tissue is mainly solid Extra Cellular Matrix includes various organic constituents like collagen, proteoglycans, and other non-collagenous proteins and chondrocytes.

### **1.1 Structure and function of Articular Cartilage**

Articular cartilage is divided into four different zones termed as the superficial, middle (or transitional), deep (or radial), and calcified zones. Non-homogeneous distribution of cells and ECM in mature articular cartilage differentiates it into different zone that contributes to the different functional properties of articular cartilage.

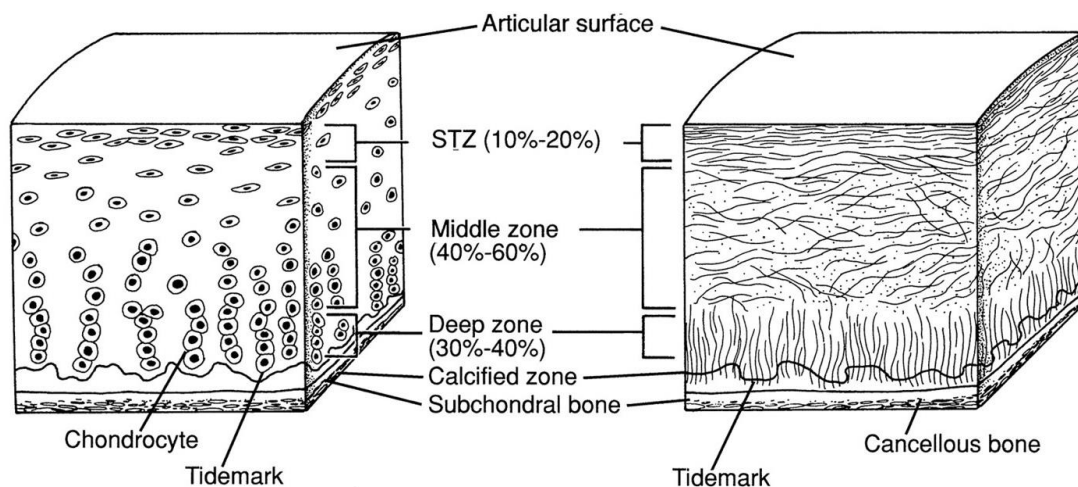


**Figure 1:** Schematic cross sectional diagram of healthy articular cartilage.

<http://ajs.sagepub.com/content/26/2/309>.

Articular cartilage is composed of different zones based on the shape of the shape of the chondrocytes and orientation of type II collagen. Superficial zone only accounts for 10–20% of the total articular cartilage thickness; consist of Type II collagen orienting parallel to the joint with flattened chondrocytes and sparse proteoglycans. The composition and organization of this zone contributes to tensile strength, resists shear during articulation, and adjusts fluid permeability. Intermediate zone or middle zone is the thickest zone consists of round chondrocytes and abundant proteoglycans with randomly arranged type II collagen. Deep layer or basal layer has highest concentration of proteoglycan with type II collagen arranged perpendicular to the joint. The functional role of these collagens is to strengthen the bond between cartilage and bone. Transitional zone is the calcified zone with collagen type X, which helps in cartilage mineralization and provides structural integrity.

## 1.2 Composition of Articular Cartilage

Articular cartilage is composed of 70–80% of water reserved in the form of stable macromolecular gels. The other 20–30% represents the Extracellular matrix (ECM) and chondrocytes.

### **1.2.1 Chondrocytes**

Chondrocytes is the only cell type having a round or polygonal morphology, but depending on its position within the articular cartilage it can also have a flattened or discoid morphology. They produce and maintain the cartilaginous matrix, which consists mainly of collagen and proteoglycans. The major metabolic pathway of chondrocytes is the anaerobic glycolysis. Due to the avascular nature of the cartilage, the physicochemical conditions of the immediate pericellular environment of the chondrocytes appear to play a critical role in regulating cell activity (Rebecca E. Wilusz et al., 2015). The chondrocytes are the source of many cytokines and growth factors important in the regulation of cartilage metabolisms. These cytokines, vitamins (ascorbic acid), hormones (insulin), or growth factors (TGF- $\beta$  (transforming growth factor b), IGF (insulin like growth factor), BMP (bone morphogenetic protein) can influence chondrogenic differentiation and phenotype (Pierre Weiss et al., 2010). Chondrocytes are responsible for the synthesis, the maintenance, and the renewal of the ECM.

### **1.2.2 Extracellular Matrix (ECM)**

Articular cartilage contains two major classes of proteoglycans, one is large aggregating proteoglycans monomers or aggrecans and the other small proteoglycans including decorin, biglycan, and fibromodulin (Poole et al, 1996; Roughley et al., 2006). Proteoglycans consist of a protein core with one or more hydrophilic glycosaminoglycans (GAG) chains. GAG found in cartilage include hyaluronic acid (HA), chondroitin sulfate, keratan sulfate, heparan sulfate, and dermatan sulfate.

Collagen is the most abundant structural macromolecule in ECM, which makes up about 60% of the dry weight of cartilage. Type II collagen represents 90% to 95% of the collagen in ECM and forms fibrils and fibers intertwined with proteoglycan aggregates. Collagen types I, IV, V, VI, IX, and XI are also present but contribute only a minor proportion, were these minor proportions of collagens help to form and stabilize the type II collagen fibril network.

The molecular organization of collagen and proteoglycans all have profound effects on the intrinsic mechanical properties of the extracellular matrix and the fluid

transport and diffusional properties of the cartilage. Proteoglycans forms huge aggregates that trapped in the collagen network. Because of their numerous negatively charged sulfate groups, these proteoglycan aggregates attract cations, which in turn bring in water to minimize differences in osmotic pressure (Alice J. Sophia Fox et al., 2009).

### **1.3 Mechanical properties of articular cartilage**

The amount of shock and energy that can be absorbed by the articular cartilage during normal activities is higher than the surrounding muscles, ligaments and tendon or even bone. The collagen fibrils are the main contributors to the tensile properties of articular cartilage. The tensile properties vary significantly among zones due to different collagen organization. A human knee joint cartilage has the equilibrium tensile modulus value higher in the superficial zone (10.1 MPa) when compared with the other zones (e.g., 5.4 MPa in the middle zone) (Akizuki S et al., 1986). While the compressive moduli of cartilage change with the depth and location. It has been reported that the compressive modulus increased nearly 27-fold from the superficial zone ( $0.079\pm 0.039$  MPa) to the deepest zone ( $2.10\pm 2.69$  MPa) in bovine articular cartilage (Schinagl RM et al., 1997).

### **1.4 Articular cartilage injuries**

Articular cartilage defects, caused by traumatic destruction or degenerative joint diseases, are predominantly divided into two categories, partial-thickness and full-thickness cartilage defects. Partial-thickness defects only damage the zonal articular cartilage but do not penetrate into the underlying subchondral bone. This blocks the blood cells, bone cells, and progenitor cells to reach defect site which inhibits the self-healing responses. Full-thickness (or osteochondral) defects penetrate the entire thickness of articular cartilage, and reach into the subchondral bone. But unlike partial-thickness defects, mesenchymal progenitor cells, macrophages, and blood cells can reach the injured site which could fasten the healing processes.

## 1.5 Surgical treatment of Articular Cartilage damages

**Microfracture** is one of the most common methods to treat small articular cartilage defects (e.g.,  $< 2 \text{ cm}^2$ ). This method creates microfractures in the underlying subchondral bone via drilling, shaving, or abrasion for the subchondral bone to release bone marrow progenitor cells to repair the defect. These are mostly applicable in the young patients due to presence of abundant mesenchymal cells. But in some cases, the generated hyaline cartilage may turn over into weaker fibrocartilage, resulting in the failure of surgery.

**Autologous Chondrocyte Implantation** or ACI is another method recommended for patients who have cartilage lesions between  $1 \text{ cm}^2$  and  $12 \text{ cm}^2$ . ACI harvest a small piece of articular cartilage from the patient's knee, further expanded *in vitro* for 3–5 weeks then reimplanted to repair the injury. But, ACI procedures need long recovery time and multiple surgeries.

In **Autologous mosaicplasty** technique to get an osteochondral autograft, healthy cartilage tissues are collected from a patient's own body and are then implanted into defect sites to reinstate the function. Though immunorejection can be prevented by using patients own cells it can result in donor site morbidity, surface mismatch or graft instability.

**Total or Partial joint replacement** is used to replace the damages part. Artificial implant composed of a metal or a polymer piece is implanted to replace the damaged joint.

**Nonsurgical treatments** are also available to treat cartilage injuries. Drugs like anti-inflammatories, COX-2 inhibitors and cortisone provide relief from symptoms of defective cartilage by suppressing an immune response. Non-steroidal anti-inflammatory drugs (NSAIDS) work by blocking the effect of enzyme cyclooxygenase. This prevents prostaglandins, the lipid compounds that cause swelling and pain during arthritis or bursitis. But NSAID can cause unwanted side effects like stomach irritation, headache, drowsiness, high blood pressure, and dyspepsia. Cortisone injections also have side effects that it should not be repeated more than few times a year, as they can weaken the tendons and softens the cartilage.

It can also suppress the body's immune system. However glucosamine sulphate and chondroitin sulphate are dietary supplements intended to slow down and reverse the degenerative mechanisms of cartilage wear. But further investigations of larger cohorts of patients for longer periods of time are needed to assess before they will be accepted into primary treatment plan for cartilage.

### **1.6 Limitations of current surgical methods for cartilage repair**

Possible limitations in the current methods of cartilage repair are mainly due to the lack of integration of the chondrocytes within the existing cartilage. This is possibly due to the insufficient capacity of implanted cells to recapitulate the complex events resulting in the native organization of the cartilaginous tissue. The lack of integration may be due to the incomplete differentiation of chondroprogenitor cells. Mesenchymal stem cells have been proposed as a potential source of cells for cell-based cartilage repair due to their self-renewal ability and multi-lineage differentiation. Though cell-based therapies have proved their feasibility there is no superiority over other surgical methods in the long run. This highlights the crucial need for optimizing various combinations of cell types, scaffolds or other chondrogenic factors.

The ideal cell-carrier substance should be the one which most closely mimics the natural environment in the articular cartilage matrix. It has been shown that cartilage-specific extracellular matrix (ECM) components such as type II collagen and glycosaminoglycan (GAG) play a critical role in regulating expression of the chondrocytic phenotype and in supporting chondrogenesis both in vitro and in vivo (Robert A. Kosher et al., 1973). Else, chondrocytes may undergo de-differentiation and produce an inferior fibrocartilaginous matrix rich in type I collagen. This inferior matrix then leads to a failure to form hyaline cartilage (K. von Der Mark et al., 1977). Thus, the selections of biomaterial in cartilage tissue engineering include biocompatibility and biomechanical strength. These features may deliver appropriate environment essential for engineered cells to regenerate a long-lasting hyaline cartilage in the defect site.

## 1.7 The concept of ‘Tissue Engineering’

The term ‘tissue engineering’ was officially coined at a National Science Foundation workshop in 1988 to mean ‘the application of principles and methods of engineering and life sciences toward the fundamental understanding of structure-function relationships in normal and pathological mammalian tissues and the development of biological substitutes to restore, maintain or improve tissue function’. The field relies extensively on the use of porous 3D scaffolds to provide the suitable environment for the regeneration of tissues and organs. This combination of cells, signals and scaffold is often referred to as a tissue engineering triad. These scaffolds essentially seeded with cells and frequently growth factors, or exposed to biophysical stimuli in the form of a bioreactor; a system that can apply different types of mechanical or chemical stimuli to cells. These cell-seeded scaffolds are either cultured *in vitro* to synthesize tissues which can then be implanted into an injured site, or are implanted directly into the injured site, using the body's own systems. This combination of cells, signals and scaffold is often referred to as a tissue engineering triad. (Fergal J.O Brien et al., 2011)

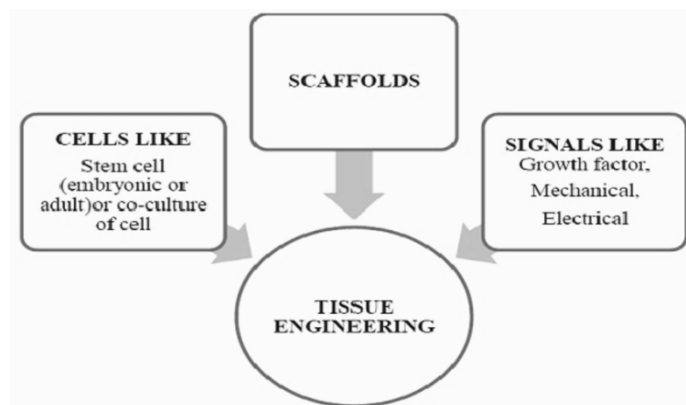


**Figure 2:** Tissue engineering triad of cells, signals and the scaffold which acts as a template for tissue formation by allowing cells to migrate, adhere, and create tissue.

The major advantage of tissue engineering approach is that tissues can be reconstructed to closely match the needs of patient’s requirements and can be transplanted into patient’s body with minimal surgical intervention, which eventually

confers several limitations encountered in the traditional tissue transplantation procedures.

Tissue engineering can develop engineered constructs which enable cartilage regeneration by providing mechanical, biological and chemical support. The use of scaffold as a substrate to support the growth of chondrocytes has given promising results. The mechanical and biochemical properties of scaffold can be manipulated to make it more efficient. Scaffolds designed to repair damaged articular cartilage for use in cell-based therapies should ideally deliver the following characteristics: (i) a three-dimensional (3D) highly porous structure to support cell attachment, proliferation and extra-cellular matrix (ECM) production and also to promote nutrient and waste exchange. ii) Mechanical properties that match with the tissues at the site of implantation. (iii) a biocompatible and bioresorbable substrate with controllable degradation rates (iv) and a reproducible structure which promote the formation of native tissue.

Both natural and synthetic polymers have been used for scaffold fabrication. Natural polymers are preferred over synthetic polymers as they are more cell friendly and promote better cell material interactions. But major disadvantages in the case of natural polymer are the lack mechanical stability, uncontrolled degradation and non-reproducibility. There is also concern for the purity of these polymers during isolation and the risk of pathogen transfer. In such cases biodegradable synthetic polymers offer a number of advantages over natural polymers. Main advantage includes the ability to tailor mechanical properties and degradation kinetics to suit various applications. Hydrogels are very good candidates in tissue engineering applications because they can fill irregularly filled shaped defects, and incorporate cells and other bioactive materials as they are more cell friendly.

Scaffold processing techniques like fiber bonding, gas foaming, membrane lamination, melt molding, temperature-induced phase separation, particulate leaching and solvent casting are used for the development of porous scaffolds. Recently design driven approach has more prominence. Rapid prototyping allows the researchers to

design the desired properties with reproducibility via computer-aided design (CAD) models and computer-controlled tooling processes (CAM).

### 1.8 Tissue engineering of Cartilage- An upcoming treatment modality

The articular cartilage has an important role in protecting the underlying bone from damage as a result of weight bearing and allowing smooth movements by reducing friction. The concept of a tissue engineering approach to cartilage repair was first proposed by William Green MD in 1977. He was the first to use the rabbit as a model to study cartilage repair. He used decalcified bone as a type of scaffold for cell transplantation. Clinical application of such a tissue engineering approach was first attempted by a Swedish group with fair-to-excellent clinical results in their clinical subjects (J.K. Francis Suh et al., 2000).

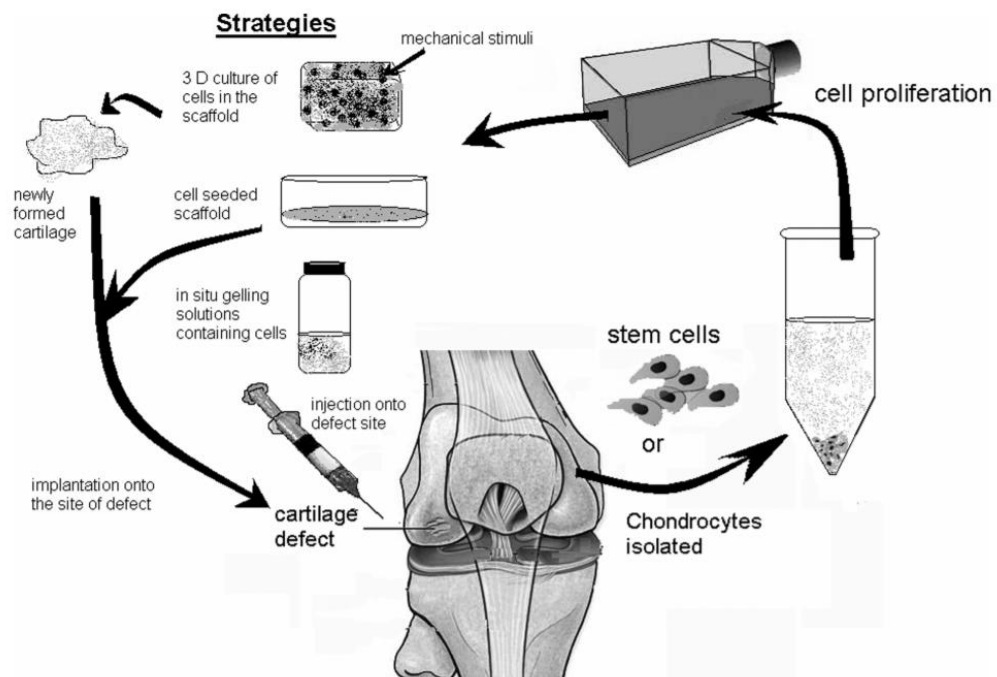


**Figure 3:** Schematic representation of methods of cartilage tissue engineering

The elementary principle of cartilage tissue engineering involves isolation of cells that may be expanded in vitro and then either encapsulated in a three-dimensional network for proliferation or mixed with in situ gelling systems and subsequently injected into

site of injury. Cells can be acquired by culturing primary autologous/heterologous chondrocytes, mesenchymal stem cells, or from embryonic stem cells.

Scaffolds are meant to preserve cell infiltration, proliferation, and subsequent differentiation in response to signalling molecules and mechanical stimulation and provide initial mechanical strength. Chondrocytes are highly environment specific, and it has been found that the interaction of integrin receptors with chondrocytes results in the production of extracellular molecules such as type II collagen and aggrecan (Schmidt M. B et al., 2006). Ideal properties of a cartilage tissue-engineering scaffold include biocompatibility, promotion of cell differentiation and neocartilage formation, porous structure, mechanical stability, adherence and integration with the surrounding native cartilage, and proper filling of the defect site (Biji Balakrishnan et al., 2018)

The selection of biomaterial is crucial to the success of tissue engineering approaches in cartilage repair. Biomaterials including natural or synthetic, biodegradable or non-biodegradable, have been introduced as possible cell-carrier substances, one that can closely mimics the naturally occurring environment in the articular cartilage matrix for cartilage repair.

### **1.9 Natural polymers for cartilage regeneration**

Alginate is a biodegradable polysaccharide derived from brown seaweed. Alginate gels are found to stimulate the differentiation of bone marrow and adipose tissue derived stromal cells towards a chondrogenic phenotype. This possibly may due to the lack of cellular interactions or limited oxygen and nutrient supply inside alginate hydrogels. But they lose mechanical property in vitro due to an outward flux of ions into the medium (Schoichet et al., 1996).

Fibrin hydrogels is formed using enzyme catalysed crosslinking of fibrinogen at room temperature in the presence of thrombin, calcium chloride, and factor XIIa, are readily available from patients' blood and have been approved for clinical use. The major drawback of fibrin glue is their low mechanical stability, limiting their role in load bearing applications. Studies showed that fibrin chondrocyte construct have been

observed to degrade before proper formation of cartilaginous tissue. ( Fusseneger et al., 2003)

Hyaluronic acid gels are obtained by the esterification of biocompatible and biodegradable hyaluronate. They are one of the components of proteoglycan in the extracellular matrix. However, the gels often contain impurities and remain mechanically weak compromising their use in skeletal tissue engineering.

Collagen is also a component present in ECM and it is expected to produce most suitable conditions for chondrocytes. Among the different types of collagen, collagen type II showed greater chondrogenic activity. But the use of collagen gels remains limited because of qualitative batch variations and loss of shape (Diduch et al., 2000). Gelatin is derived from collagen successfully used in cell and drug delivery. Gelatin hydrogels are weak at physiological temperature but can be made better in combinations with stiffer solid scaffolds.

### **1.10 Synthetic polymers**

Most widely used synthetic degradable polymers comprise a class of polyesters like poly (lactic acid) (PLLA), poly (glycolic acid) (PGA) and their copolymer poly (lactic-co-glycolic acid). Poly(glycolic acid) is a long standing, well studied scaffold for engineering stem-cell-derived cartilage, but degrades at a faster rate and is weaker than most synthetic scaffolds (Grande et al., 2003).

Poly ( $\epsilon$ - caprolactone) (PCL) is another FDA approved biocompatible polyester that have been widely explored for tissue engineering applications. PCL have sufficiently long degradation time of 2 years but the degradation can be tailored by blending with other polymers. Novel degradable PCL networks, PLGA/PCL/PLGA tri-block copolymers and PCL-chitosan matrices are more hydrophilic, degrade faster and possess desirable mechanical properties as compared to PCL ( Kweon et al., 2003, Sarasam et al., 2005).In general the biocompatible synthetic polymers have been generally acceptable for load bearing applications. PCL with high mechanical stability is found to be very favourable for cartilage tissue engineering than the commonly employed polyesters like PLA, PGA and PLGA.

## 1.11 Hydrogels

Hydrogels are group of polymeric materials, were the hydrophilic structure gives them capable of holding large amounts of water in their three-dimensional networks. An ideal cell carrier material should be one that closely mimics the naturally occurring matrix in the articular cartilage environment. Hydrogels have a similar macromolecular structure to cartilage, which is a highly hydrated tissue composed of chondrocytes embedded in type II collagen and GAGs. Thus, cartilage is an obvious tissue to engineer using hydrogel scaffolds. (Jeanie L. Drury et al., 2003)

Hydrogels based on biopolymers can mimic characteristics of the natural ECM and thus have the potential to direct the migration, growth, and organization of cells during tissue regeneration. Biopolymers used for hydrogel scaffold development for cartilage tissue engineering comprise of polysaccharides such as hyaluronate, chondroitin sulfate chitosan, alginate, and agarose and proteins such as silk fibroin, fibrin, and collagen.

Some of the inadequacies of traditional hydrogels are poor mechanical properties and slow response time to external stimuli. Currently there are several methods which can improve the mechanical stability of the hydrogels. These methods include crosslinking, blending with other polymers and by forming interpenetrating polymer networks (IPNs) with other mechanically strong polymers, which will result in good mechanical properties and high degree of swelling for the hydrogel without collapse.

A variety of synthetic and naturally derived materials are used to make hydrogels. Synthetic materials include poly(ethylene oxide) (PEO), poly(vinyl alcohol) (PVA), poly(acrylic acid) (PAA), poly(propylene fumarate-co-ethylene glycol) (P(PF-co-EG)), and polypeptides. Though hydrogels derived from biopolymers show remarkable benefits over synthetics, exclusively with respect to cell signaling, they lack flexibility in designing specific properties such as porosity and mechanical strength. But one can readily control and manipulate the macrostructure, porosity, mechanical strength, and degradation time for a synthetic polymer. The concept of combining synthetic materials with naturally derived biomaterials has received great attention. These hybrid materials can have the features of both natural and synthetic

biomaterials like controllable mechanical and degradation properties, reproducibility on large-scale productions, and good processability, as well as the specific biological activity of naturally derived materials.

The microenvironment in 3D hydrogel culture might mimic the cell-to-matrix interactions or the cell-to-cell contacts of chondrocytes in native cartilage. Thus prevent dedifferentiation of chondrocytes and supports chondrocyte proliferation and matrix secretion.

### **1.12 3D printing for creating cartilage constructs**

Three-dimensional (3D) printing is a manufacturing method in which objects are made by fusing or depositing materials—such as plastic, metal, ceramics, powders, liquids, or even living cells—in layers to produce a 3D object. (Lipson H et al., 2013). This process is also referred to as additive manufacturing (AM), rapid prototyping (RP), or solid free-form technology (SFF).

3D printing was first described in 1986 by Charles W. Hull. Hull later founded the company 3D Systems, which developed the first 3D printer, called a “stereolithography apparatus.” Later in 1988, 3D Systems introduced the first commercially available 3D printer, the SLA-250. 3D printing has been used by the manufacturing industry for decades, primarily to produce product prototypes. They use fast 3D printers called “rapid prototyping machines” to create models and molds. Many of these printed objects are comparable to conventionally manufactured items.

A number of conventional manufacturing techniques were applied to fabricate porous 3D scaffolds, such as fiber bonding, phase separation, solvent casting, particulate leaching, membrane lamination, molding, and foaming. However, all these methods have major drawback: These techniques do not allow the control of scaffold architecture, pore network, or pore size. The three most commonly used 3D printer technologies in medical applications are: selective laser sintering (SLS), thermal inkjet (TIJ) printing, and fused deposition modeling (FDM).

3D-printing methods (also recognized as rapid prototyping, solid free-form fabrication, or additive manufacturing) are used to fabricate modified scaffolds with

controlled pore size and structure. All 3D printing processes offer advantages and disadvantages. Among the forty different 3D-printing techniques in development, stereolithography, fused deposition modeling (FDM), selective laser sintering (SLS), inkjet printing and colorjet printing appeared to be the most popular, due to their ability to process plastics.

During the second decade of this field (2003–2012), the number of studies in the arena of 3D printing for tissue engineering rapidly multiplied. Several studies have been come up for the scaffold design, process modelling and optimization, comparisons of 3D-printing methods, new scaffold materials for 3D printing processing, characterization of 3D printed scaffolds, *in vitro* and *in vivo* applications of 3D printed scaffolds, new 3D-printing methods for scaffold fabrication, and even the branching out of an entirely new field—3D bioprinting, or organ printing.

Fabrication of viable constructs using a novel 3D printing system provides the ability to combine synthetic polymers, which have higher mechanical strength than natural materials, accompanied by the cell growth favourable environment provided by traditional naturally-derived hydrogels. This strategy used for development of scaffolds in load-bearing tissue engineering applications, such as cartilage.

### **1.13 Polysaccharide-based hydrogels**

Polysaccharides form a class of materials which have generally been underutilized in the biomaterials field. Several factors have specifically contributed to the growth and recognition of polysaccharide-based biomaterials. First and foremost is the critical role of immune recognition of saccharide moieties in cell signaling schemes. The other factor is the need for a new material with specific, controllable biological activity and biodegradability in tissue engineering research. Apart from their biological activity, one of the more vital properties of polysaccharides in general is their capability to form hydrogels. This mechanism is strongly influenced by the types of monosaccharide involved, as well as the existence and nature of substituent groups. Proteoglycans found in articular cartilage consist of a core protein and covalently attached GAG chains. The cartilage specific GAGs include chondroitin 4-sulfate (glucuronic acid and *N*-acetyl-galactosamine with an SO<sub>4</sub> on the 4-carbon position),

chondroitin 6-sulfate (glucuronic acid and *N*-acetyl-galactosamine with an SO<sub>4</sub> on the 6-carbon position) and keratan sulfate (galactose and *N*-acetyl-glucosamine with an SO<sub>4</sub> on the 6-carbon position). GAGs assume a flexible rod conformation, and unstable in solution results in poor intrinsic gel formation properties. But another GAG, hyaluronic acid (glucuronic acid and *N*-acetyl-glucosamine) is different from other GAGs. Purified hyaluronic acid is used as a structural biomaterial because of its high molecular weight and gel forming ability. Ethyl and benzyl esterified hyaluronate membranes have demonstrated excellent healing responses and biodegradability in vivo (Campoccia D et al., 1996). Hyaluronic acid and derivatives have been used as therapeutic aids in the treatment of osteoarthritis as a means of improving lubrication of articulating surfaces and thus reducing joint pain (Iwata S. et al., 1993, Frizziero L et al., 1998). Evaluating particular importance of GAGs in stimulating the chondrogenesis, use of GAGs or GAG analogs as components of a cartilage tissue scaffold appears to be a logical approach for enhancing chondrogenesis (Kosher R A et al., 1973).

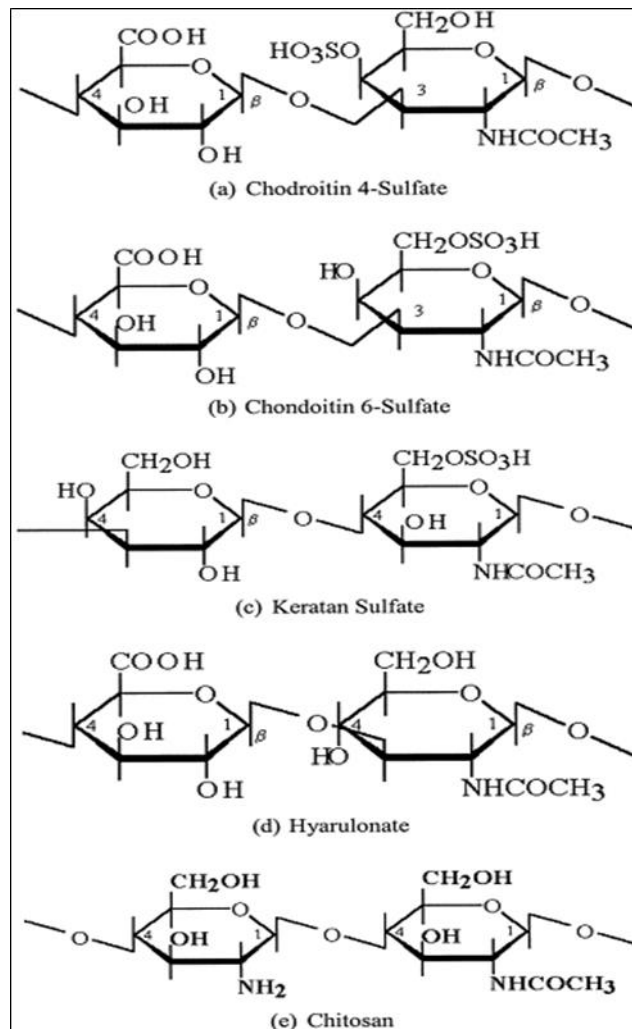


**Figure 4:** Molecular structures of the polysaccharide repeating units (J. K. Francis Suh et al., 2000)

### 1.13.1 Chitosan in cartilage regeneration

Among all of the polysaccharides known chitosan has been widely accepted as a natural biomaterial for tissue regeneration applications. Chitosan has been widely investigated for biomedical applications such as tissue engineering, controlled drug and protein delivery and non-viral gene delivery. Chitosan is a polycationic polysaccharide comprising glucosamine and *N*-acetylglucosamine residues. As glycosaminoglycans (GAGs) may play a special role in modulating chondrocyte morphology, and their differentiation and function (Bhardwaj et al., 2011), biomaterials that are structurally analogous to GAGs, such as chitosan, seem suitable candidates for tissue engineering of cartilage (Roughley et al., 2006). It thus shares

some characteristics with various GAGs and hyaluronic acid present in articular cartilage. Depending on the preparation procedure and source, chitosan's average molecular weight may range from 50 to 1000 kDa with degrees of deacetylation ranging from 50 to 90%. The polymer has been extensively studied for industrial applications based on the films and fiber formation (Rathke TD et al., 1994).

Chitosan shares some characteristics with various GAGs and hyaluronic acid present in articular cartilage. The potential benefits of chitosan compared with any other synthetic polymers are its chemical similarity and ability to interact with the GAGs present in cartilage. So the use of chitosan based cartilage tissue scaffold appears to be a logical approach for enhancing chondrogenesis. Moreover, chitosan can be enzymatically degraded *in vivo* by lysozyme a polycationic protein present in the ECM of human cartilage (Jonathan M. Moss et al., 1997). The charge density allows chitosan to form insoluble ionic complexes with a wide variety of anionic polymers such as GAGs and alginates (Takahashi T et al., 1990, Gaserod O et al., 1998), as well as synthetic polyanions such as poly (acrylic acid) (Denuziere A et al., 1998). Because the chitosan charge density is pH dependent, this property can be used as a technique for local delivery of biologically active polyanions such as the GAGs and DNA (Leong KW et al., 1998, Mac Laughlin FC et al., 1998). Chitosan based scaffold's can be processed into porous structures for use in cell transplantation and tissue regeneration.

A number of researchers have observed the tissue response to various chitosan-based implants. These materials have been found to induce a minimal foreign body reaction. Formation of normal granulation tissue, often with accelerated angiogenesis appears to be the typical course of healing. In the short term, a significant accumulation of neutrophils in the vicinity of the implants is often seen, but this dissipates rapidly. On the whole all these stimulatory effects on immune cells play a role in inducing local cell proliferation and eventually integration of the implanted material with the host tissue.

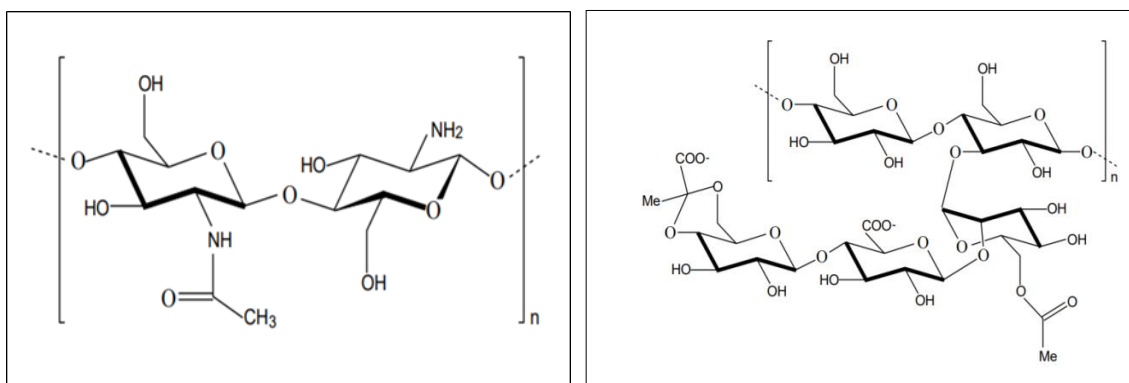


**Figure 5:** Chemical structures of A) chitosan and B) xanthan gum

### 1.13.2 Xanthan Gum in cartilage tissue engineering

Xanthan gum (XG) is a type of sugar that is made from a bacterium called *Xanthomonas campestris*, through a process of fermentation. It is commonly used as a thickening and stabilizing agent in both food and medicine. It is also used as emulsifier, suspension stabilizer, flocculant, gelling and viscosity agent. XG is a high molecular weight exo polysaccharide having branched polymeric chains with excellent biocompatibility and good water-solubility. The primary structure of XG consists of pentasaccharide subunits, comprises of D-glucosyl, D-mannosyl, and D-glucuronyl acid residues in a 2:2:1 molar ratio with varying proportions of O-acetyl and pyruvyl residues.

XG in combinations with hydroxyapatite, bioactive glass, chondroitin sulphate and chitosan has been already tried for various biomaterial applications. XG can gellify in situ within seconds, to retain large quantities of water, and thus to offer a similar environment to that of natural ECM (Khang et al., 2012, Dyondi et al., 2013).

The carboxyl groups present in xanthan gum, when combined with the amine groups in chitosan, create a microenvironment that favors the stabilization of proteins and allows formation of hydrogels (Dyondi et al., 2013, Izawa et al., 2014) and tablets (Popa et al., 2010). Studies have showed that Gellan/xanthan gels loaded with chitosan nanoparticles, basic fibroblast growth factor (bFGF), and bone morphogenetic protein 7 (BMP-7) stimulated the differentiation of human fetal osteoblasts.

The Chitosan-xanthan gum based hydrogel can be prepared as microspheres, films, particles, beads, and sponges, depending on the desired use. Their effective polyelectrolyte gel formation capability has been investigated for the drug delivery applications with least immune responses (Fatiha Chellat et al., 2000).

#### **1.14 Hypothesis**

*An injectable two component chitosan/xanthan gum dialdehyde hydrogel supporting the growth of chondrocytes may be a viable option as a bioink for 3D printing of cartilage constructs.*

#### **1.15 Objectives**

- To synthesize chitosan-xanthan gum dialdehyde based hydrogel for cartilage tissue engineering.
- To characterize the physicochemical properties of the chitosan-xanthan gum dialdehyde gel prepared in three different ratios.
- To analyse the cytocompatibility of prepared hydrogel.
- To assess the functionality and viability with chondrocytes.

#### **1.16 Significance of the study**

3D printing is an advanced evolving technology that allows for the creation of organized 3D tissue constructs via a “layer-by-layer” deposition process. The high spatial resolution of 3D bioprinting which is an automated, computer aided deposition of cells, biomaterials and growth factors has the potential to replicate complex native like tissue architecture which is very important in terms of the functionality associated with the system. Major challenges in 3D printing cartilage are the fabrication of scaffold which is printable and capable of maintaining structural, biomechanical and functional properties of native cartilage. Here we have fabricated two component natural polysaccharide based CH-XDA hydrogel which can closely mimic the native cellular environment and in future which could be manipulated as a bioink for the creation of layered articular cartilage system.

## CHAPTER 2

### MATERIALS AND METHODS

#### 2. Materials

Chitosan~ 75% deacetylated, (Mn-70,000-90,000) by GPC (Sigma Aldrich, USA), xanthan gum (E415) (Urban platter, INDIA) was used for this study. Dialysis tubing (Spectra/Por® Dialysis Tubing, M.W.C.O 12000) is from spectrum laboratories Inc. CA, USA. For cell culture experiments, Dulbecco's Modified Essential Medium – High glucose (DMEM-HG), Fetal Bovine serum (FBS), Phosphate buffered saline (PBS), Antimycin-Antimycotic, and 0.25% trypsin-EDTA were procured from Invitrogen, USA. Collagenase II and Live dead assay kit were procured from Invitrogen and DMMB dye from Sigma Aldrich, USA).

#### 2.1 Preparation of Xanthan gum dialdehyde

Xanthan gum was oxidised to form Xanthan gum dialdehyde using periodate oxidation technique. Briefly, 1gm of XG was dissolved in 100 ml of distilled water and the required amount of periodate was added to obtain 100% oxidised xanthan gum dialdehyde. The reaction was allowed to proceed in dark for overnight at 25 °C with constant stirring. The solution was then dialysed against distilled water 3-4 days with three changes of water every day to remove the whole periodate from the solution. The dialysate was then freeze dried and stored at -20°C in the dark. The % oxidation was confirmed by Hydroxylamine hydrochloride assay (Diana Paiva et al., 2016) and the reaction was confirmed by NMR analysis.

##### 2.1.1 Determination of Degree of Oxidation

The degree of oxidation was determined by the hydroxylamine hydrochloride titration method which is defined as the number of oxidized units per 100 elementary units. It was determined by the reaction of hydroxylamine hydrochloride with oxidized xanthan gum. This reaction produces hydrochloric acid, which is then titrated with NaOH and related to the aldehyde content in oxidized xanthan gum. The degree of oxidation was calculated according Equation (1), where  $V_{\text{NaOH}}$  is the

consumed volume of NaOH at the equivalence point,  $C_{\text{NaOH}}$  is the concentration of NaOH solution (0.1 M),  $N_{\text{C=O}}$  is the possible number of aldehyde groups,  $m$  is the dry weight of oxidized XG (0.1 g) and  $M$  is the molecular weight of the repeating unit of XG (934 g/mol). In the case of xanthan gum, eight aldehyde groups can be formed per repeating unit by the cleavage of the C–C bond between adjacent –CHOH groups.

$$\text{Degree of oxidation} = \frac{V_{\text{NaOH}} \times C_{\text{NaOH}}}{N_{\text{C=O}} \times m/M} \times 100 \quad (1)$$

### 2.1.2 Nuclear Magnetic Resonance spectroscopy

<sup>1</sup>H nuclear magnetic resonance (NMR) spectra of xanthan gum and oxidised xanthan gum were recorded on a Bruker Avance III 400 spectrometer (Bruker Optik GmbH, Ettlingen, Germany), operating at frequencies of 400 and 100 MHz, respectively, using D<sub>2</sub>O (Deuterium oxide) as solvent. Chemical shifts were expressed in (ppm), relative to the resonance of trimethylsilyl propanoic acid (TMSP) (0.00 ppm) as an internal standard.

### 2.2 Preparation of chitosan- xanthan gum dialdehyde (CH-XDA) hydrogels

For preparing CH-XDA hydrogels, for preparing the hydrogel 2% chitosan was prepared by dissolving in 0.075% acetic acid. 2.5% of xanthan gum solution prepared by dissolving in PBS solution. Neutralisation of gel was done by using HEPES buffer. Three gel composition prepared by mixing two components in the ratios shown in Table 1.

**Table 1:** Composition chart of hydrogels prepared.

Sample	Composition	Chitosan( $\mu$ l)	Xanthan gum dialdehyde( $\mu$ l)
A	80:20 CH-XDA	80	20
B	75:25 CH-XDA	75	25
C	70:30CH-XDA	70	30

## 2.3 Characterization of the chitosan-xanthan gum dialdehyde based hydrogel

### 2.3.1 FT-IR analysis

Fourier Transform Infrared Spectroscopy (FT-IR) provides information about the specific chemical groups of the materials. FT-IR spectrum of mm thickness samples were recorded at room temperature in the room temperature in the range of 5000- 500  $\text{cm}^{-1}$  region using BRUKER optic GmbH.

### 2.3.2 Percentage degree of crosslinking

Ninhydrin assay is used to determine free amine groups present in the gel to comparing it with the uncrosslinked chitosan. 1 mg of sample was boiled with freshly prepared ninhydrin reagent at 100<sup>0</sup>C for 1hr. After boiling the solution was cooled and 1ml of ethanol was added to stabilize the colour formed. The optical absorbance of solution was measured at 590nm with spectrophotometer (Varian Cary 50 uv vis spectrophotometer). Glycine at various known concentrations was used as standards. The amount of free amino group is proportional to optical absorbance of the solution. Triplicate samples were used for determining the % degree of crosslinking.

The degree of crosslinking of the solution is calculated using equation

$$\% \text{ degree of crosslinking} = \frac{C_i - C_f}{C_i} \times 100$$

$C_i$  is optical absorbance of bare chitosan solution.  $C_f$  is optical absorbance of crosslinked gels.

### **2.3.3 Gelling time determination of chitosan-xanthan gum dialdehyde gel**

Gelling time was determined by measuring the viscosity change during the gelation between chitosan and oxidised xanthan gum using a programmable viscometer (Brookfield) at approximately  $20 \pm 2$  °C and 30 rpm using a small sample adapter and spindle number S25. Gelling time was determined as the time at which the viscosity of mixture begins to increase sharply and reaches a maximum value.

### **2.3.4 Percentage gel fraction**

To determine the percentage gel fraction, freeze dried hydrogels of 5mm and 2 mm thickness was immersed in deionised water for 16hr at room temperature and then sample was again freeze dried and the insoluble dried sample was again weighed.

The gel fraction measured using formula,

$$\% \text{ Gel fraction} = \frac{W_d}{W_i} \times 100$$

$W_i$  is the initial weight of dried sample and  $W_d$  is the weight of dried insoluble part after extraction. Triplicate samples were used in this study.

### **2.3.5 Degree of swelling**

The study was performed to understand the water holding capacity and stability of the hydrogel. For this study freeze dried hydrogel of 5mm diameter and 2 mm thickness weighed and immersed in PBS (pH 7.4) and kept in pre-weighed containers for known intervals of time. The samples withdrawn at regular intervals and wet weight measured.

$$\% \text{ Degree of swelling} = \frac{\text{Final weight} - \text{Initial weight}}{\text{Initial weight}} \times 100$$

### **2.3.6 Rheological studies**

The rheological properties of the gels in three ratios were carried out by modular compact rheometer (Anton Paar , MCR 102, NIIST). A cone plate with cone diameter of 24 mm and a cone angle of 2.009 ° was used and the measurement gap was fixed at 0.105mm. A plate with a diameter of 40 mm combined with a thermostat was used to maintain the temperature at 25 °C. The oscillation frequency was set at 10 rad s<sup>-1</sup> and applied shear stress at 2 Pa. The dynamic viscoelastic functions such as the dynamic shear storage modulus (G') and loss modulus (G'') were measured as a function of time, temperature or angular frequency.

## **2.4 CYTOTOXICITY ANALYSIS USING L929 CELLS**

### **2.4.1 Direct contact test**

To assess the cell compatibility of the gel system, L929 cells seeded at a density of 5000 cells per cm<sup>2</sup> onto a 6 well plate culture plate until the cells became 75% confluent. The gel is placed on to confluent cell layer and observed after 24 hours in direct contact. While cells grown on a culture plate without any gel taken as a control. Images were taken using phase contrast microscope (Olympus1X71).

### **2.4.2 Test on extract (MTT ASSAY)**

The cell viability was evaluated by test on extract or MTT assay. 100 µl of Chitosan-Xanthan gels of three different ratios were prepared and kept in extraction medium (DMEM) at 37<sup>0</sup> C for 24 hr. L929 cells were seeded in a 96 well plate at a density of about (5X10<sup>3</sup> cells per well) and were incubated for 24 hr at 37C with 5% CO<sub>2</sub>. 100%, 75%, 50% and 25% of extract was taken for each of the three ratios to make the total volume 100 µl with DMEM and added to the well plate after removing the cell medium. Cells incubated with DMEM alone were kept as the control. After 24 h of incubation with the extract the extract was removed and incubated with 10 µl of mg/ml MTT solution for 3 hr. MTT was removed completely and then 100 µl of

DMSO was added to each well to solubilise the formazan crystals formed. Optical density was measured at 540nm with the use of (ASYS UVM 340).

$$\text{Percentage viability} = \left[ \frac{\text{Absorbance of extract treated}}{\text{Absorbance of the control cells}} \right] \times 100$$

## **2.5 Isolation of chondrocytes from rabbit articular cartilage**

Rabbit articular joints were cut open aseptically and cartilage pieces scrapped out and washed in PBS. The cartilage pieces were digested in digestion media containing DMEM, Collagenase type II 0.2% (w/vol), penicillin (100U/ml), streptomycin (100µg/ml) and fungizone (1 µg/ml) for 6 hr at 37 °C. The collagenase action inactivated by adding FBS containing media and centrifuged at 1800rpm for 5 minutes to get chondrocyte pellet which was then resuspended in DMEM with serum medium and seeded into 25cm<sup>2</sup> flasks and incubated at 37 °C, 5% CO<sub>2</sub> until confluent. Medium was changed every 2-3 days following which the confluent monolayer was trypsinized using 0.25% trypsin-EDTA solution. Cells from passage 2-4 were used for the study.

## **2.6 Encapsulation of chondrocyte in CH-XDA hydrogels**

Approximately 2X10<sup>6</sup> chondrocytes per 100µl of cells were pelleted down and resuspended in HEPES neutralised 30 µl XDA solution. This solution was mixed with 70 µl neutralised chitosan to form the cell encapsulated hydrogel. The 70:30 composition was used for all the cell culture studies based on the MTT assay results. The gel with cells was then transferred into complete medium and cultured for a period of 7, 14, and 21 days at 37 °C and 5% CO<sub>2</sub>. At the end of the culture period samples were retrieved and assessed.

## **2.7 Live dead staining**

The cell viability and the pattern of growth at different periods of time assessed using Live/Dead Viability/Cytotoxicity kit (Invitrogen, Molecular probes Eugene, Oregon, USA). Hydrogels retrieved after 7, 14, and 21 days incubated in PBS containing 4mM calcein-AM which stains the live cells green and 2mM ethidium bromide which

stain the dead cells red. The images were taken using a fluorescence microscope (Leica Generic) and the cell distribution in 21 day was assessed using Z stacked generated images through Confocal microscope (Olympus Fluoview FV3000)

## **2.8 Quantification of Total glycosaminoglycan content**

Samples retrieved after each time points of culture period washed with PBS and then lyophilised. The lyophilised sample was weighed and digested with papain at 65<sup>0</sup>C for 3 hr. Samples centrifuged at 10000 rpm for 10 minutes at 20<sup>0</sup> C and supernatant was used to estimate GAG content using DMMB assay. Blank, standard and test were used for analysis. To each well of 96 well plates, 50 µl of sample followed by 150 µl 1 X DMMB reagent was added and OD measured at 525nm.

## **2.9 Safranin O staining and Toluidine blue staining**

Cryosections were washed with distilled water and nucleus stained with Harris hematoxylin for 5 minutes. Excess stain was removed with alcohol followed by bluing with tap water. Counter stained the sections with 0.2 % FCF and washed with .05% acetic acid. The sections were incubated in 0.1% safranin O for 5-15 minutes. After washing and air drying, sections are viewed and imaged under microscope (Leica DM 4000M).

In addition, evaluation of the chondrogenic differentiation was carried out by staining 21 day scaffold construct with Toluidine blue. Cells were fixed in 10% formalin for 30min, washed 2 times with PBS and stained with 0.1% Toluidine blue for 30min in order to highlight the presence of proteoglycans and subsequently the level of chondrogenic differentiation.

## **2.10 Immunofluorescence analysis**

Cell constructs were rinsed in PBS thrice, then fixed in 4% formalin for 4 h, followed by washing with PBS. Fixed samples were incubated with primary antibodies of anti-collagen II (1:100 dilution) kept at RT for overnight. After washing with PBS, samples were incubated with a goat anti-mouse IgG antibody-FITC conjugate (1:200 dilution). DAPI (Sigma-Aldrich) was used for nuclear staining. Images were recorded using an inverted confocal laser scanning microscope (Olympus Fluoview FV3000)

### **2.11 3D printing using the Chitosan Xanthan gum dialdehyde as ink**

3D printing with Chitosan-XDA gel system was performed at room temperature in an extrusion based printer system. The various parameters for the printing process like the extrusion pressure, moving print speed, filament gap and needle gauge was standardised for the printing process.

## CHAPTER 3

### Results and Discussion

#### 3.1. Characterization of chitosan-xanthan gum dialdehyde (XDA) hydrogels

Cartilage is a challenging tissue to engineer using hydrogel scaffolds as it is composed of 70–80% of water retained in the form of a stable macromolecular gels. Cell-ECM interaction plays a major role in determining the regeneration potential of cartilage tissue. Currently, research is being directed to cell therapy associated with specific scaffold-like hydrogels. Articular cartilage, in particular, is considered to be a good candidate for tissue engineering, because it requires less metabolic involvement due to lower cellularity and avascular matrix.

The extracellular matrix (ECM) and chondrocytes represent 20–30% of the articular cartilage. Given the significance of GAGs in stimulating the chondrogenesis, the use of GAGs or GAG analogs as components of a cartilage tissue scaffold seems to be a logical approach for enhancing chondrogenesis. Chitosan is one such GAG analog frequently used in pharmaceutical applications, as it shows unique properties, including bioactivity, biocompatibility and biodegradability. The idea of making xanthan gum based hydrogel is also not new. Xanthan gum has been used in a wide range of contexts, ranging from food to cosmetics and pharmaceuticals. It can be combined with other polysaccharides to produce films, gels, or solutions with better mechanical properties. Main attraction is that it can produce high viscous solution at very low concentration. Chellat et al. has showed that a combination of these two natural polysaccharides, xanthan–chitosan based hydrogels are recognized as promising candidates for targeted delivery and controlled release of encapsulated products for oral administration because degradation causes the production of only non-toxic metabolites and the complex has relatively high enzymatic resistance (Chellat et al., 2000).

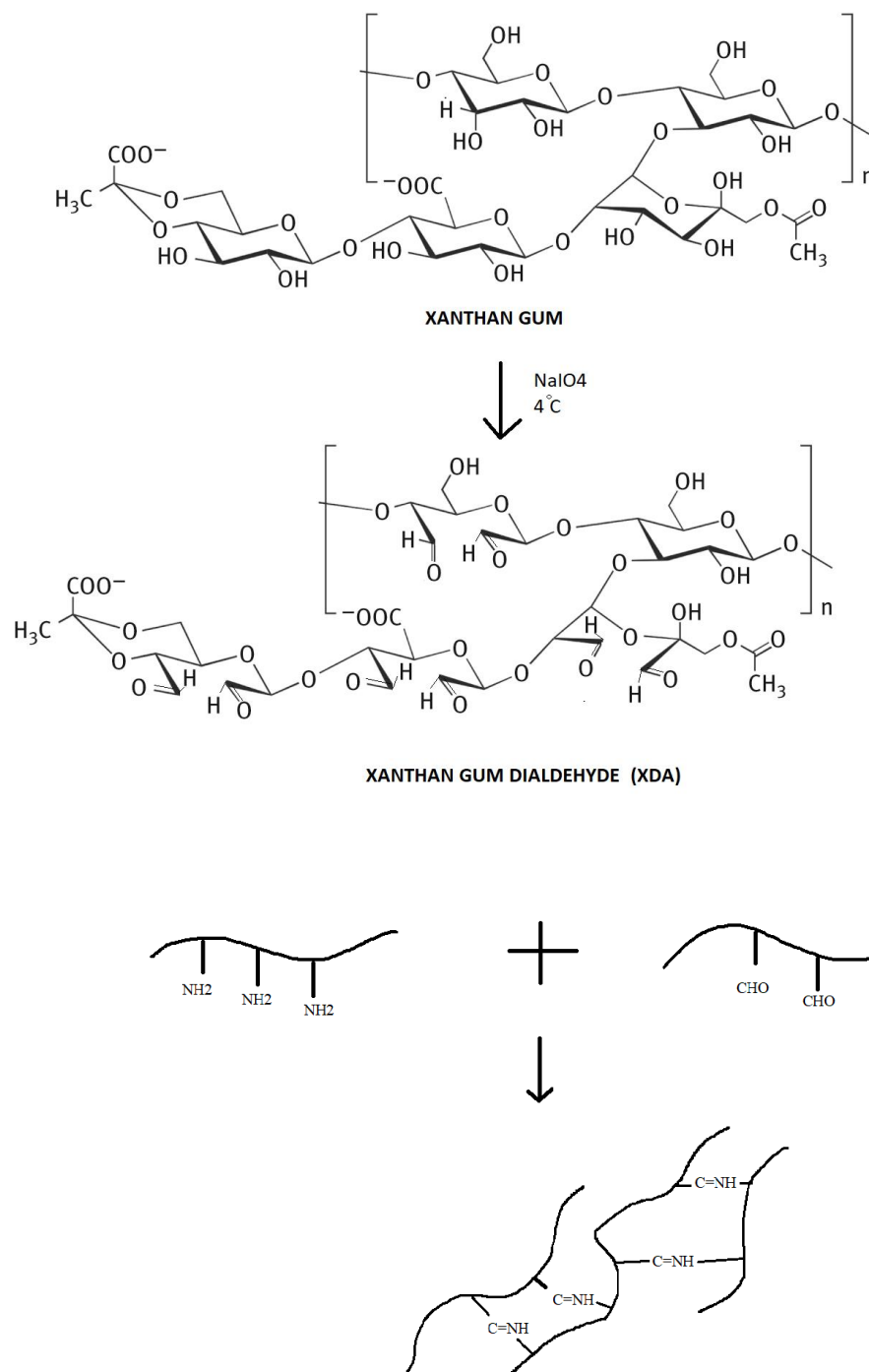


**Figure 6:** Schematic representation of the formation of CH-XDA gels through Schiff's base reaction between free amine groups on chitosan and aldehyde groups on xanthan gum dialdehyde.

Various analytical tests to assess the purity of chitosan used in this study were performed previously in our laboratory and the results are shown in the table below.

**Table 2:** Test for chitosan (Sigma Aldrich, Cat No. 3646)

<b>Test for Chitosan (Sigma Aldrich, Cat No. C3646)</b>			
Batch No. SLBC2867V, SLBL3564V, 068K00751			
<b>Sl No-</b>	<b>Item</b>	<b>Specification</b>	<b>Results</b>
<b>1</b>	Viscosity Measurement of Chitosan	150-200 cP	195±5 cP
<b>2</b>	Molecular Weight of Chitosan (Mw)(GPC)	-	550 KDa
<b>3</b>	Dry Matter content of Chitosan	≥95 %	99.9 ± .0.03%
<b>4</b>	Protein Assay for Chitosan	≤0.1 %	0.06± .03%
<b>5</b>	Degree of deacetylation of chitosan	≥ 75 %	85 ± 2 %
<b>6</b>	Insoluble Content of Chitosan	≤ 0.2 %	0.1 ± .05%
<b>7</b>	Heavy Metals Content of Chitosan		
	Arsenic (As)	< 0.5 ppm	< 0.0530 ppm
	Lead (Pb)	< 40 ppm	< 0.0420 ppm
	Cadmium (Cd)	< 0.5 ppm	< 0.0027 ppm
	Mercury (Hg)	< 0.2 ppm	< 0.0610 ppm

The application of other microbial polysaccharides such as gellan gum has been reported in the literature for the encapsulation of human chondrocytes for cartilage regeneration (Ana C. Mendes et al., 2012) but the use of oxidised xanthan gum with chitosan as cell encapsulation matrix is a new concept which we have tried to explore. The reaction basically involves the formation of Schiff's base between free amine groups on chitosan and dialdehyde group on Xanthan gum thereby leading to a crosslinked structure. Schiff's base crosslinking reaction can occur at room temperature and does not require any chemical initiator to activate the reaction. Moreover the cationic chitosan and anionic Xanthan gum can form an ionic crosslinked structure which can contribute to stable gel formation.

The main aim of the study was to develop a fast gelling hydrogel with good stability, the gel formation was through Schiff's base formation between chitosan and Xanthan gum aldehyde. Xanthan gum was modified to xanthan gum dialdehyde by periodate

oxidation. The experimental design was aimed for a 100% oxidation. To assess the degree of oxidation hydroxylamine hydrochloride assay was performed where the degree of oxidation was calculated from Equation to be  $44.75 \pm 1.7 \%$  ( $n=3$ ). The confirmation of the oxidation was done using NMR and FTIR. Xanthan gum is a polysaccharide with pentasaccharide repeating unit composed of D-glucose, D-mannose, D-glucuronic acid, acetal-linked pyruvic acid, and O-acetyl groups. Oxidation takes place by the C–C cleavage between (–CHOH)<sub>2</sub> groups to form dialdehydes. The major NMR peaks at 1.5 ppm in Figure (7b) depicts the methyl group of the pyruvated group and 1.8 ppm the acetated group. The corresponding peaks that confirms the oxidation reaction is shown Table 3 given below.

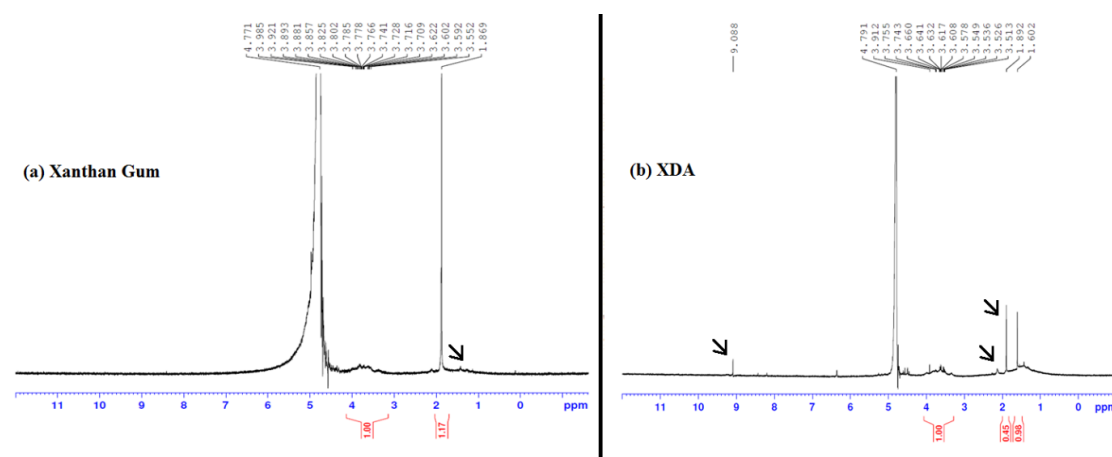


**Figure 7:** <sup>1</sup>H NMR spectrum showing a) xanthan gum and b) xanthan gum dialdehyde

The reaction was also confirmed from the FTIR Plot (Figure 8). Xanthan gum showed the characteristic peaks of OH stretch at  $3288 \text{ cm}^{-1}$ , CH stretch at  $2909 \text{ cm}^{-1}$ , the C=O at  $1600 \text{ cm}^{-1}$ , characteristic COO- at  $1407 \text{ cm}^{-1}$ , OH bending at  $1027$ . The main peak at  $1153 \text{ cm}^{-1}$  is attributed to the C-O bond stretching of the C-OH group. On oxidation the XDA sample shows a decrease in the C=O peak at  $1604 \text{ cm}^{-1}$  with the introduction of CH stretch at  $2922 \text{ cm}^{-1}$  and  $2854 \text{ cm}^{-1}$ . The characteristic C-O bond stretching of

the C-OH group also disappears after the oxidation is completed which confirms the reaction.

**Table 3 :** Relevant spectroscopic data ( $^1\text{H}$  NMR) of oxidized xanthan gum in  $\text{D}_2\text{O}$ .

Peak values (ppm) $\delta$	Peak Assignment
1.602	Methyl group of the oxidized pyruvated mannose
1.898	The methyl group on the acetylated group
1.4	CH <sub>3</sub> on pyruvated mannose
2.2	CH <sub>3</sub> of oxidized acetylated mannose
6.4	CH ethylenic carbon of mannose after $\beta$ elimination
9.088	H-C=O of mannose after $\beta$ elimination

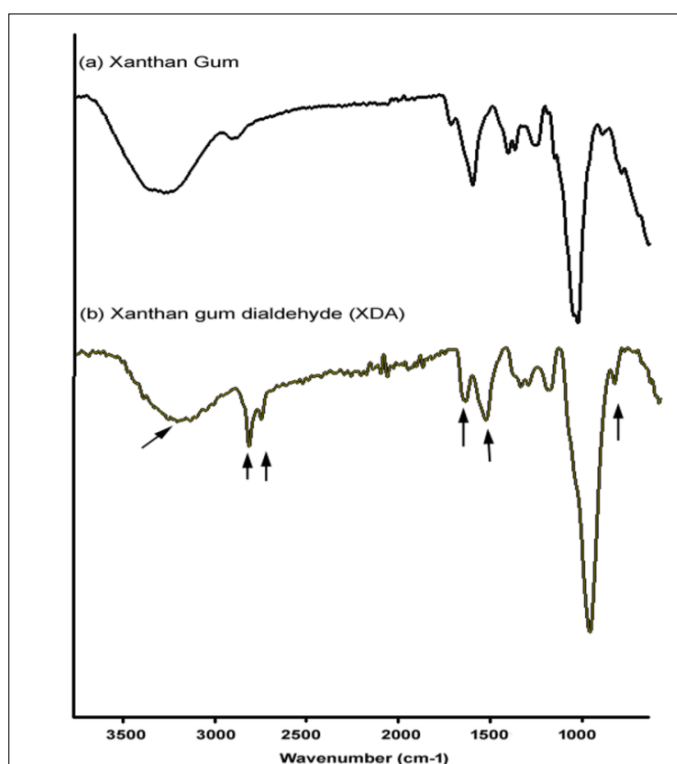


**Figure 8 :** FTIR plot of a) xanthan gum and b) xanthan gum dialdehyde

Different combinations of chitosan and xanthan gum ratios tried in order to see the dependency of concentration of two components. Faster and stable gel formation was occurring when the chitosan concentration was increased. Concentration ratios beyond 30 volume ratio of xanthan gum dialdehyde with chitosan led to stiffer non uniform gels to be formed. Hence we restricted this study to three different ratios within this range so as to get a uniform and stable gel. Concentration ranges were 80:20 CH-XDA, 75:25 CH-XDA, 70:30 CH-XDA. The characteristic peaks in all the three ratios showed C=N at  $1630\text{ cm}^{-1}$ , NH stretch at  $3286\text{ cm}^{-1}$ , NH bending at  $1555\text{ cm}^{-1}$  and the characteristic CH stretch at  $2920\text{ cm}^{-1}$ . It is seen that as the ratio of the oxidized xanthan gum is increased the intensity of the CN stretch at 1630 increases. As the ratio of the chitosan component increases the NH stretch is seen to increase (80:20 CH-XDA > 75:25 CH-XDA > 70:30 CH-XDA). This confirms the Schiff's base formation in the three ratios that were prepared.

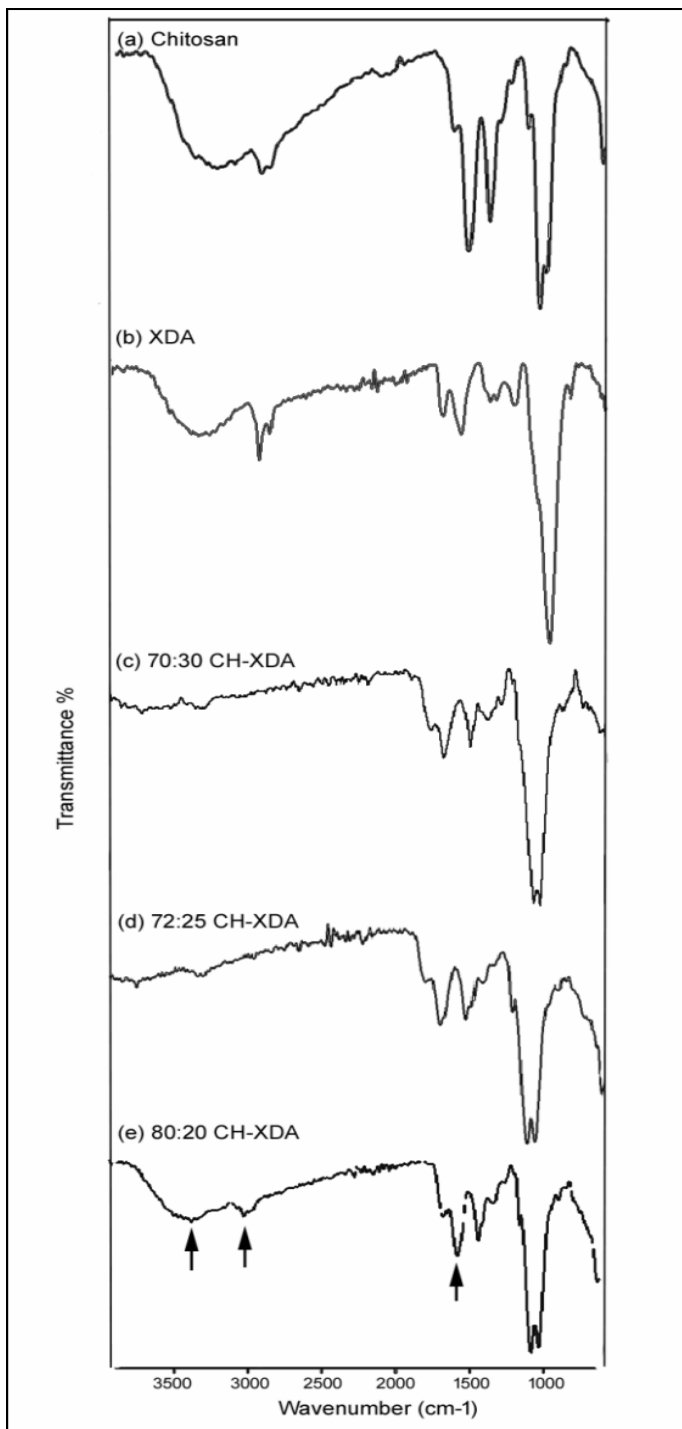


**Figure 9** : FTIR plot showing a)chitosan; b)xanthan gum; c) 70:30 CH-XDA; d) 75:25 CH-XDA; e) 80:20 CH-XDA

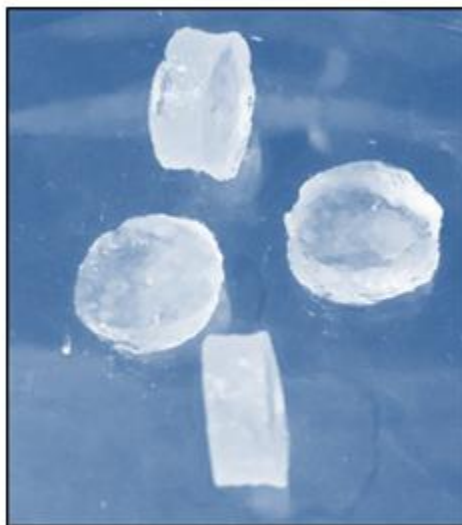


**Figure 10 :** Gels made of 70:30 CH-XDA composition

Studying the degree of swelling of hydrogels is crucial to understand the behaviour of hydrogel in retaining the amount of fluid. The property of swelling is important in maintaining the hydrated state of a cell for proper nutrient and waste exchange and also for the diffusion of signalling molecules, which are critical to cellular viability when encapsulated. Since cartilage is an avascular tissue nutrient uptake depends totally on the diffusion process. Generally the swelling ratio of the gels first increase rapidly with increasing swelling time and then tries to stabilize until equilibrium reached. The significance test showed that swelling is not much varied among the three ratios tried ( $p > 0.05$ ). Only 30-35% swelling capacity was observed for the three ratios selected which may be attributed to the crosslinked structures due to schiffs base formation and the presence of four pairs of dialdehyde groups in one molecule leading to small crosslinks within the structure and hence a tighter crosslinking intramolecularly contributing to lower swelling ratios.

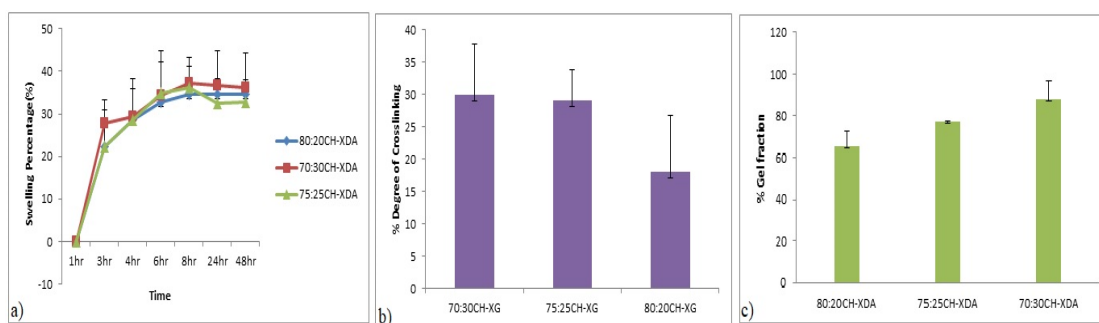


**Figure 11:** a) Degree of swelling of three different ratios for a period of 48 hr; b) % Degree of crosslinking; C) % gel fraction. (Mean±SD) (n=3).

The stiffness and stability of hydrogel is related to degree of crosslinking happened between chitosan and xanthan gum. The percentage degree of crosslinking was determined by assessing the free amine groups in the hydrogel. Concentration of free amine groups in the chitosan decreased after crosslinking with the xanthan gum. The % degree of crosslinking was found almost same for 70:30 CH-XDA ( $29.9 \pm 7.90$ ) and 75:25 CH-XDA ( $29.1375 \pm 8.6$ ) combinations. While the 80:20 CH-XDA combination has shown only  $18. \pm 4.7$  percentage degree of crosslinking. There is no significant difference ( $p > 0.05$ ) observed between the three different combinations. The swelling and crosslinking studies have showed that gel formation is almost interdependent on such small variation of concentration difference for Chitosan and Xanthan gum. Also the low values for crosslinking density in the three ratios may be attributed to the fact that the chitosan used in this study had only about 75% degree of deacetylation which is an indirect measure of the number of free amine groups in the sample and only 45% of effective oxidation of the Xanthan groups for effective crosslinking. However the decreased values of the swelling inspite of the low crosslinking density may be attributed to the fact that the crosslinks may be formed within the same xanthan gum molecule as there is possibility of four dialdehyde group formation within the same molecule which may limit the swelling efficiency.

Gelling time was also evaluated in the three hydrogel formulations. Faster gelling was observed in the 70:30 CH-XDA gel compositions ( $18.28 \pm 1.3$  seconds) where the

crosslinking was higher and the gels were getting strong and stable with time. (Figure 11). The other two compositions were also getting gelled at  $21.08 \pm 2.5$  seconds and  $20.76 \pm 2.3$  seconds respectively. The gelling time decreases when the volume ratio of xanthan gum dialdehyde is increased. The % gel fraction also proves that the gel formed is comparatively more stable when the volume ratio of xanthan gum dialdehyde is increased.

Rheological properties needs to be studied to assess the viscoelasticity of the gel which a very crucial parameter. Usually the measurement of the strain amplitude dependence of the storage and loss moduli ( $G'$ / $G''$ ) is done to characterize viscoelastic behavior. Here a strain sweep is done on all the three ratios of gels right after the two components are placed together in the sample cell. Usually in a viscoelastic gel, on providing the strain the storage modulus will be higher than the loss modulus, ie the material behaves solid like and is highly structured. On increasing the strain above a critical strain results in the disruption of the network structure. As the gel undergoes the crosslinking reaction the molecular weight of the polymer increases with increase in viscosity and there is a critical transition point or the cross-over point where the elastic and viscous moduli are equal ( $G'=G''$ ). Here in all the three ratios  $G' > G''$  indicating the strength of gels. In 80:20CH-XDA gels, below 10% strain which is the critical strain, the structure is intact. Above the critical strain the structure is disrupted and material becomes more fluid like. Similarly the 75:25 CH-XDA gel also shows a critical strain value at 10.1%. However, on increasing the XDA content in the 70:30 CH-XDA gel the critical strain is around 2.52% which shows that at this ratio the linear viscoelastic region is at a lower strain. This understanding of the linear viscoelastic region is necessary to study the response of the gel towards various processing effects especially since we are looking at the printability of the gel. More studies needs to be performed to do a complete study of the gel mainly the frequency sweep curve and the study of power law index to determine the Non Newtonian behavior of the gel system which is being studied further.

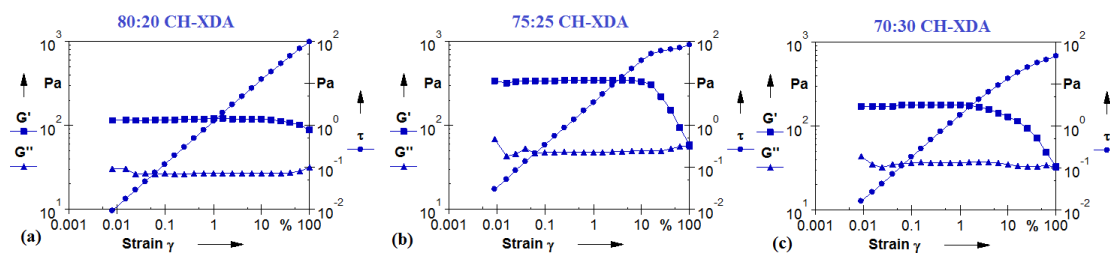


**Figure 12:** Rheological properties of CH-XDA hydrogel prepared in three different ratios.

### 3.2 Biological evaluation of the Chitosan-Xanthan gum dialdehyde hydrogel

Direct contact test is a primary *in-vitro* cell cytotoxicity assay, performed to show an initial confirmation that the scaffold does not elicit any harmful effects on the cell viability. The three different combinations were placed on a monolayer of L929 cells for 24 hours. It was seen that all the three samples did not elicit any harmful leachants and the cells maintained their characteristic spindle shaped morphology. The cells were well spread and properly attached to the substratum as like control cells.

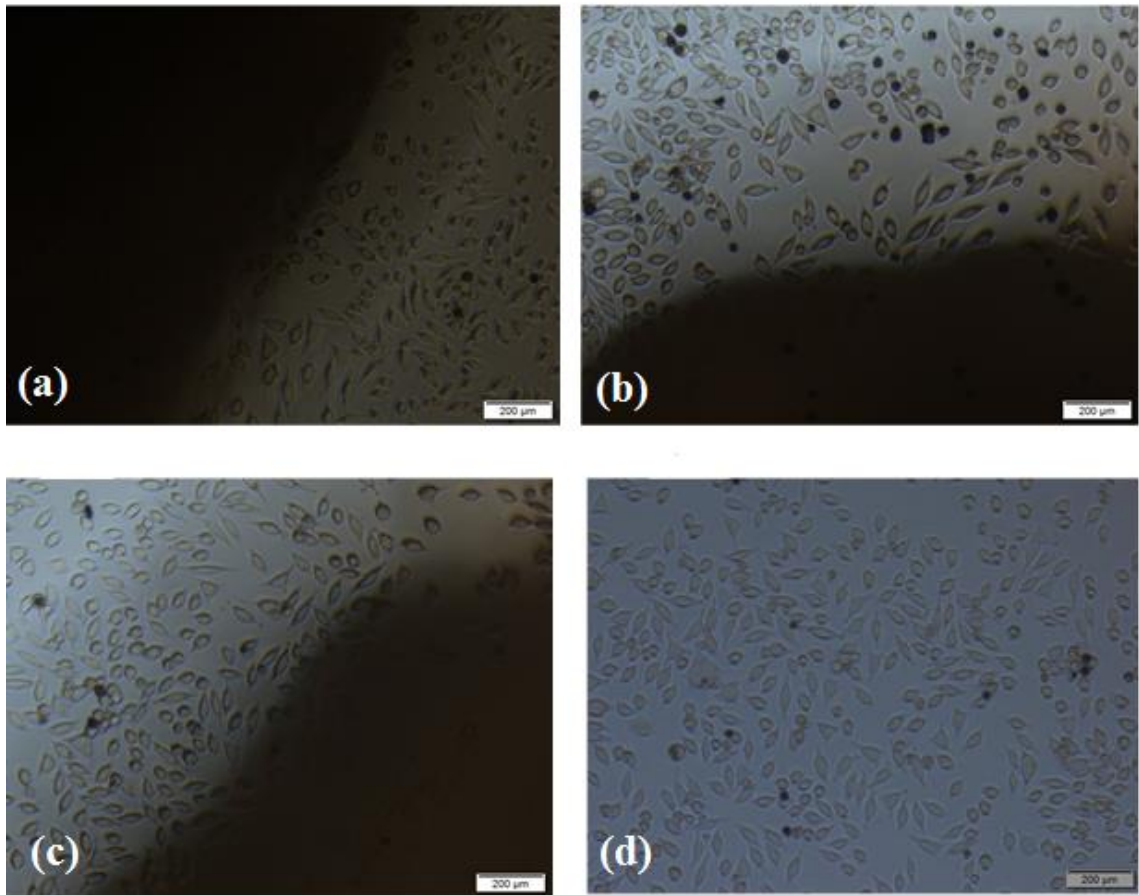


**Figure 13:** Microscopic images of Direct contact assay. a) 75:25 CH-XDA b) 80:20 CH-XDA c) 70:30 CH-XDA and d) Control after 48 hr

The non-cytotoxicity of the scaffold was further confirmed by treating the monolayer of L929 with extracts of scaffold for a period of 24hr. The cell viability assay showed that no harmful leachants are produced by Chitosan xanthan gum dialdehyde hydrogel system. Among the 3 combinations tried 70:30 CH-XDA was showing increased percentage viability compared to other combinations. Neither chitosan concentration nor Xanthan gum dialdehyde concentration affects the properties of the cell, however we chose 70:30 CH-XDA as our final working concentration based on the percentage cell viability assay which is an indication of cell proliferation too and the gelation time.

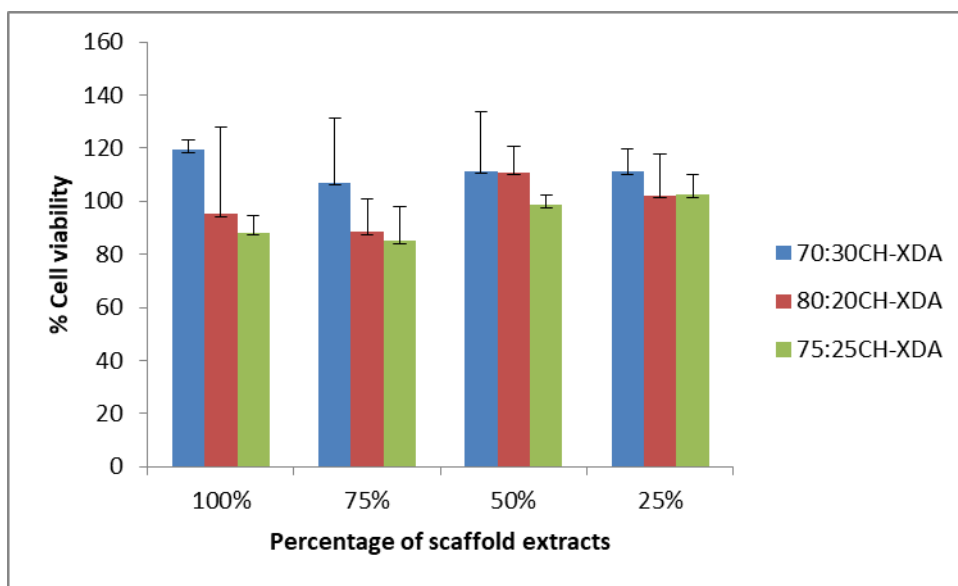


**Figure 14:** Assessment of mitochondrial activity by MTT assay.

### 3.3 Chondrocyte encapsulation CH-XDA gel system

Having found that material is non-cytotoxic, it was further used for chondrocyte encapsulation studies. Chondrocytes were isolated from rabbit articular cartilage and the cells of passage 2-4 were used for the studies. We attempted both explant culture and direct tissue digestion using enzymes to isolate chondrocytes. Cells were subcultured to passage 3 before they were used for the encapsulation studies. Chondrocytes were encapsulated within gels and cultured for period of 7, 14 and 21 days. To assess the viability of encapsulated cell within the CH-XDA scaffold live dead assay was performed on 7, 14 and 21 day retrieved samples. The viability of the cells on encapsulation at the different time points were assessed using Live Dead Assay kit. Live cells were distinguished by presence of intracellular esterase activity determined by the enzymatic conversion of nonfluorescent cell permeant calcein AM to intensely fluorescent green calcein. Ethidium bromide enters through damaged membranes and bind to the nucleic acid to produce bright red fluorescence in dead cells. Chondrocytes are characterized by round phenotype, which is prerequisite for efficient matrix production. Live Dead assay results confirmed that cells were viable and maintained the characteristic morphology of chondrocytes. The cell number was found to increase at day 21 and the cells were seen to uniformly distribute within the scaffold. Cluster formation of cells was seen at day 21. Spherical aggregation of

chondrocytes is evidences of increased chondrogenesis due to increased intercellular contacts.

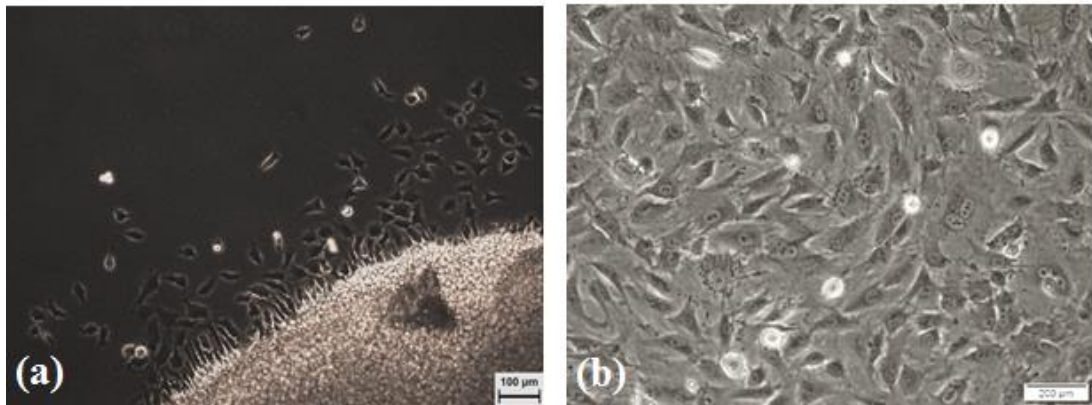


**Figure 15:** Cells isolated of rabbit articular cartilage: a) from explants ; b) after digestion.

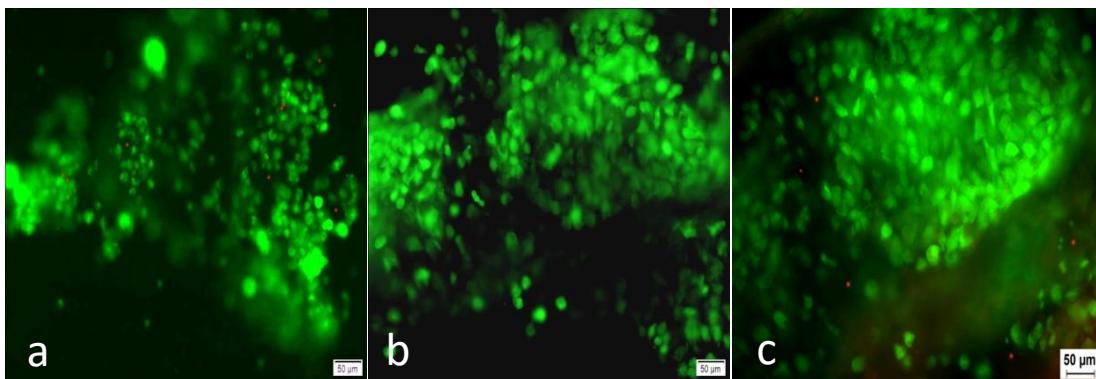


**Figure 16:** Live Dead assay of encapsulated chondrocyte on : a) 7; b) 14 and c) 21 days of culture in CH-XDA gel.

The ability of cartilage to withstand compressive forces is directly proportional to its GAG and collagen content, the levels of these two matrix components are a most crucial determinant of repair tissue properties. The secretion of ECM by chondrocytes in natural hydrogel matrix was assessed by estimating the glycosaminoglycan content in the scaffold system. The total sulphated GAG content was estimated by DMMB assay for the retrieved samples after 7, 14 and 21 days (Figure 18a). Results obtained

showed a significant increase in the GAG content from 7 to 21 days confirmed extracellular matrix production by chondrocytes entrapped within CH-XDA hydrogel system. The data was confirming that CH-XDA scaffold provide favourable environment for cell adhesion and in maintaining the cell morphology as well as for secreting the GAGs. Uniform distribution of cells and GAGs and proteoglycans in the ECM was visualised by Safranin O staining and toluidine blue staining and the presence of collagen content detected using collagen type II antibody staining (Figure 17 a , b, c and d).

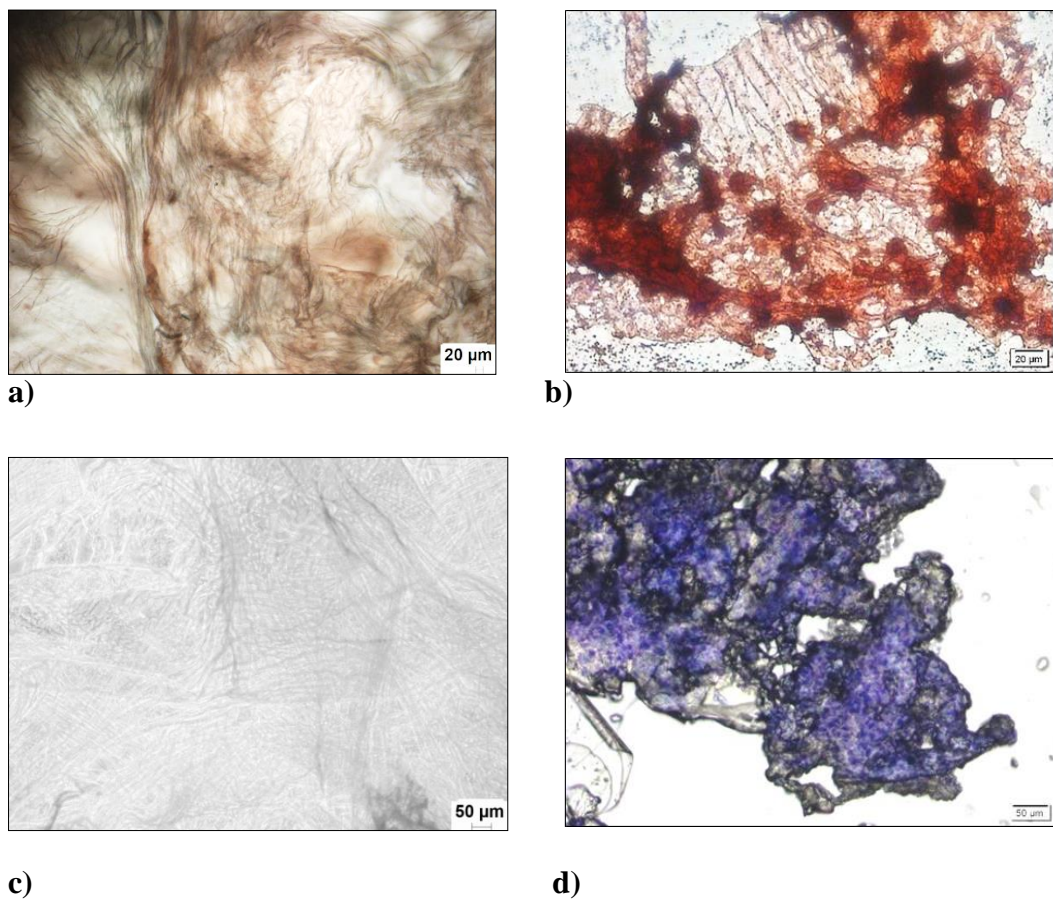


**Figure 17 :** a) Safranin O staining of control without cells b) safranin O staining of 21 day construct, which stains proteoglycans in the ECM c) Toluidine blue staining of control without cells d) Toluidine blue staining of 21 day scaffold construct to stain the proteoglycans and GAG.

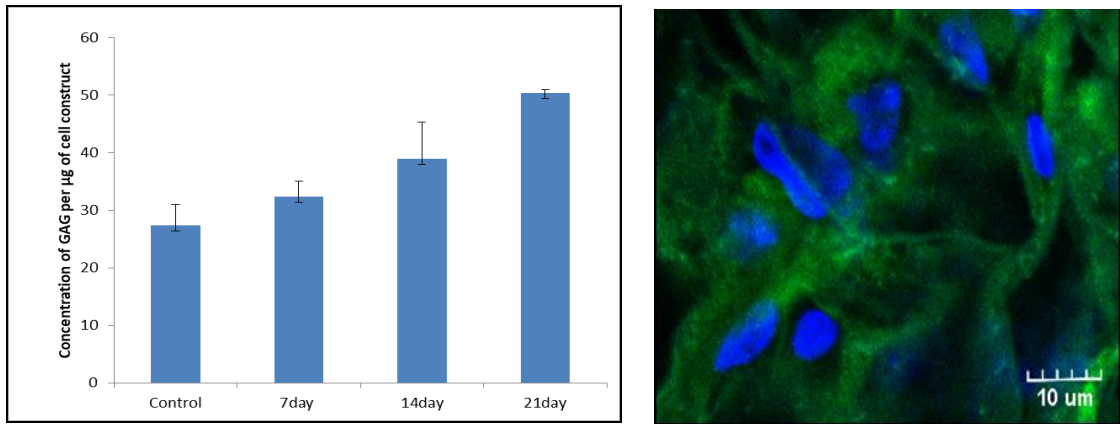


**Figure 18:** a) Quantification of total GAG content by DMMB assay for 7, 14 and 21 day culture. ( Mean  $\pm$  SD, n=3) . b) Immunofluorescence staining of 21 day construct on collagen type II antibody.

Scaffolds serve as a synthetic extracellular matrix (ECM) to establish the cells in a three-dimensional architecture and to present the stimuli, which direct the growth and formation of a desired tissue. Findings from this study also suggest that, in a static environment provided by the CH-XDA scaffold helped the cells to retain chondrogenic phenotype and promote free diffusion of nutrients and waste materials for all cells throughout the culture periods would serve as an ideal scaffold for cartilage regeneration.

Since the hydrogel system proved to work well with chondrocytes, some initial 3D printing studies were performed to standardise the print parameters. The print parameters were chosen so as to attain a smooth line print. The parameters that were standardised for this study is as shown below.

**Table 4:** Parameters standardised for 3D printing.

<b>PARAMETERS- PRINT SETTINGS</b>	
<b>Layer height</b>	0.1 mm
<b>First layer height</b>	0.1mm
<b>Fill density</b>	20%
<b>Extrusion pressure</b>	23.7 psi
<b>nozzle gauge</b>	16G
<b>Solid infill threshold area</b>	70mm <sup>2</sup>
<b>SPEED FOR PRINT MOVES</b>	
<b>Perimeters, Small perimeters ,External perimeters, infill, bridges, first layer speed</b>	1.5 mm/s
<b>PRINTER SETTINGS (Extruder)</b>	0.1mm



**Figure 19 :** The 3D printed gel composition of 90CH:10XDA

The earlier composition studied was then attempted to be 3D printed. However since all the three compositions had gelling time about 21 seconds the extrusion of these gels were seemingly difficult as they tend to gel within the syringe thereby preventing the gel from being uniformly printed hence we explored slower gelling composition of 90CH:10XDA to meet the printability requirements. However, more work is warranted in the printing of layered structures with and without cells and exploring the print quality and the viability of cells within the printed hydrogel.

Repair of injured cartilage based on the current treatment modalities faced challenges including maintenance of cartilage cells phenotype and integration of the construct with host tissue. Chondrocytes are fully differentiated cells which are responsible for the maintenance of ECM. ECM like environment could further enhance the cytocompatible nature of the hydrogel scaffolds. In that case Polysaccharide based hydrogel system can further enhance the cell signalling mechanisms inside the hydrogel. Cationic Chitosan and anionic Xanthan gum based system has ionic crosslinking along with Schiff's base formed linkages contribute a GAG analogous microenvironment within the chondrocyte encapsulated scaffold system. Thus chitosan-xanthan gum based natural polymer hydrogel system could mimic the GAG rich ECM of the articular cartilage and promotes cell adhesion and growth. Moreover the cationic chitosan can retain the negatively charged GAGs, proteoglycans and other species secreted by chondrocytes can further enhance the strength and stability of the hydrogel system. This hydrogel system ultimately proves to be a better candidate for cartilage tissue engineering and further exploring the use in the realm of 3d bioprinting will help to generate tissue specific engineered cartilage.

## CHAPTER 4

### Conclusion

Natural polysaccharide based injectable CH-XDA hydrogel system is a fast gelling, physically stable and cytocompatible scaffold system where chondrocytes can be efficiently grown and maintained. Chondrocytes retained their characteristic spherical morphology with sufficient extracellular matrix production. Future studies include using this scaffold as a bioink for the fabrication of 3D printed cartilage constructs.

### Future perspectives

Injectable materials have a great potential for the development of minimally invasive therapeutics for multiple biomedical applications. Hydrogels are of specific interest in this area, as the hydrophilic polymer structure imparts a biomimetic microenvironment, which is used to modify cellular interactions or for the delivery biological molecules. Injectable hydrogel can be used as a delivery system for therapeutic agents while designing minimally invasive strategies for treating diseases, both in vitro and in vivo. We have showed that CH-XDA gel system as a promising scaffold for cartilage tissue engineering applications. However, further studies warranted to evaluate the potential of this hydrogel system to use as a bioink for the construction of structural and functional cartilage system.

Future studies that need to be done in this area include;

- 3D printing with the CH-XDA hydrogel system encapsulating cells within it.
- To study the nature of gels over extended time points.
- To study the degradation of gels.
- To extend the study to in vivo animal models to ascertain the efficiency and functionality of the gel system.

## Reference

1. Akizuki S, Mow VC, Müller F, Pita JC, Howell DS, Manicourt DH. Tensile properties of human knee joint cartilage: I. Influence of ionic conditions, weight bearing, and fibrillation on the tensile modulus. *Journal of Orthopaedic Research*. 1986;4(4):379-92.
2. An J, Teoh JE, Suntornnond R, Chua CK. Design and 3D printing of scaffolds and tissues. *Engineering*. 2015 Jun 1;1(2):261-8.
3. Anselme K, Davidson P, Popa AM, Giazzon M, Liley M, Ploux L. The interaction of cells and bacteria with surfaces structured at the nanometre scale. *Acta biomaterialia*. 2010 Oct 1;6(10):3824-46.
4. Argin-Soysal S, Kofinas P, Lo YM. Effect of complexation conditions on xanthan–chitosan polyelectrolyte complex gels. *Food hydrocolloids*. 2009 Jan 1;23(1):202-9.
5. Baechler EC, Batliwalla FM, Karypis G, Gaffney PM, Ortmann WA, Espe KJ, Shark KB, Grande WJ, Hughes KM, Kapur V, Gregersen PK. Interferon-inducible gene expression signature in peripheral blood cells of patients with severe lupus. *Proceedings of the National Academy of Sciences*. 2003 Mar 4;100(5):2610-5.
6. Balakrishnan B, Banerjee R. Biopolymer-based hydrogels for cartilage tissue engineering. *Chemical reviews*. 2011 Mar 21;111(8):4453-74.
7. Buckwalter, J. A. “Articular Cartilage Injuries.” *Clinical Orthopaedics and Related Research*® 402 (September 2002): 21.
8. Chawla S, Kumar A, Admane P, Bandyopadhyay A, Ghosh S. Elucidating role of silk-gelatin bioink to recapitulate articular cartilage differentiation in 3D bioprinted constructs. *Bioprinting*. 2017 Sep 1;7:1-3.
9. Chellat F, Tabrizian M, Dumitriu S, Chornet E, Magny P, Rivard CH, Yahia LH. In vitro and in vivo biocompatibility of chitosan-xanthan polyionic complex. *Journal of Biomedical Materials Research: An Official Journal of The Society for Biomaterials, The Japanese Society for Biomaterials, and The*

- Australian Society for Biomaterials and the Korean Society for Biomaterials. 2000 Jul;51(1):107-16.
10. Chia HN, Wu BM. Recent advances in 3D printing of biomaterials. *Journal of biological engineering*. 2015 Dec;9(1):4.
  11. Cui X, Breitenkamp K, Finn MG, Lotz M, D'Lima DD. Direct human cartilage repair using three-dimensional bioprinting technology. *Tissue Engineering Part A*. 2012 Apr 18;18(11-12):1304-12.
  12. Da Silva MA, Crawford A, Mundy JM, Correlo VM, Sol P, Bhattacharya M, Hatton PV, Reis RL, Neves NM. Chitosan/polyester-based scaffolds for cartilage tissue engineering: assessment of extracellular matrix formation. *Acta Biomaterialia*. 2010 Mar 1;6(3):1149-57.
  13. Denuziere A, Ferrier D, Damour O, Domard A. Chitosan–chondroitin sulfate and chitosan–hyaluronate polyelectrolyte complexes: biological properties. *Biomaterials*. 1998 Jul 1;19(14):1275-85.
  14. Drury JL, Mooney DJ. Hydrogels for tissue engineering: scaffold design variables and applications. *Biomaterials*. 2003 Nov 1;24(24):4337-51.
  15. Dyondi D, Webster TJ, Banerjee R. A nanoparticulate injectable hydrogel as a tissue engineering scaffold for multiple growth factor delivery for bone regeneration. *International journal of nanomedicine*. 2013;8:47.
  16. Gao Y, Liu S, Huang J, Guo W, Chen J, Zhang L, Zhao B, Peng J, Wang A, Wang Y, Xu W. The ECM-cell interaction of cartilage extracellular matrix on chondrocytes. *BioMed research international*. 2014; 2014.
  17. Gåserød O, Smidsrød O, Skjåk-Bræk G. Microcapsules of alginate-chitosan–I: a quantitative study of the interaction between alginate and chitosan. *Biomaterials*. 1998 Oct 1;19(20):1815-25.
  18. Hamman JH. Chitosan based polyelectrolyte complexes as potential carrier materials in drug delivery systems. *Marine drugs*. 2010 Apr 19;8(4):1305-22.
  19. Hoemann CD, Sun J, Chrzanowski V, Buschmann MD. A multivalent assay to detect glycosaminoglycan, protein, collagen, RNA, and DNA content in milligram samples of cartilage or hydrogel-based repair cartilage. *Analytical biochemistry*. 2002 Jan 1;300(1):1-0.

20. Hutmacher DW. Scaffolds in tissue engineering bone and cartilage. In *The Biomaterials: Silver Jubilee Compendium 2006* (pp. 175-189).
21. Iwata H, Tanabe S, Sakai N, Tatsukawa R. Distribution of persistent organochlorines in the oceanic air and surface seawater and the role of ocean on their global transport and fate. *Environmental Science & Technology*. 1993 Jun 1;27(6):1080-98.
22. Koo Y, Choi EJ, Lee J, Kim HJ, Kim G, Do SH. 3D printed cell-laden collagen and hybrid scaffolds for in vivo articular cartilage tissue regeneration. *Journal of Industrial and Engineering Chemistry*. 2018 Jun 15.
23. Kosher RA, Lash JW, Minor RR. Environmental enhancement of in vitro chondrogenesis: IV. Stimulation of somite chondrogenesis by exogenous chondromucoprotein. *Developmental biology*. 1973 Dec 1;35(2):210-20.
24. Kweon H, Yoo MK, Park IK, Kim TH, Lee HC, Lee HS, Oh JS, Akaike T, Cho CS. A novel degradable polycaprolactone networks for tissue engineering. *Biomaterials*. 2003 Feb 1;24(5):801-8.
25. Lim SS, Vos T, Flaxman AD, Danaei G, Shibuya K, Adair-Rohani H, AlMazroa MA, Amann M, Anderson HR, Andrews KG, Aryee M. A comparative risk assessment of burden of disease and injury attributable to 67 risk factors and risk factor clusters in 21 regions, 1990–2010: a systematic analysis for the Global Burden of Disease Study 2010. *The lancet*. 2012 Dec 15;380(9859):2224-60.
26. Lipson H, Kurman M. *Fabricated: The new world of 3D printing*. John Wiley & Sons; 2013 Jan 22.
27. Loebel C, Rodell CB, Chen MH, Burdick JA. Shear-thinning and self-healing hydrogels as injectable therapeutics and for 3D-printing. *nature protocols*. 2017 Aug;12(8):1521.
28. Lohmander S. Proteoglycans of joint cartilage: structure, function, turnover and role as markers of joint disease. *Bailliere's clinical rheumatology*. 1988 Apr 1;2(1):37-62.
29. MacLaughlin FC, Mumper RJ, Wang J, Tagliaferri JM, Gill I, Hinchcliffe M, Rolland AP. Chitosan and depolymerized chitosan oligomers as condensing

- carriers for in vivo plasmid delivery. *Journal of Controlled Release*. 1998 Dec 4;56(1-3):259-72.
30. Maldonado M, Nam J. The role of changes in extracellular matrix of cartilage in the presence of inflammation on the pathology of osteoarthritis. *BioMed research international*. 2013;2013.
  31. Mandrycky C, Wang Z, Kim K, Kim DH. 3D bioprinting for engineering complex tissues. *Biotechnology advances*. 2016 Jul 1;34(4):422-34.
  32. Markstedt K, Mantas A, Tournier I, Martínez Ávila H, Hägg D, Gatenholm P. 3D bioprinting human chondrocytes with nanocellulose–alginate bioink for cartilage tissue engineering applications. *Biomacromolecules*. 2015 Apr 7;16(5):1489-96.
  33. Melchiorri C, Meliconi R, Frizziero L, Silvestri T, Pulsatelli L, Mazzetti I, Borzì RM, Uguccioni M, Facchini A. Enhanced and coordinated in vivo expression of inflammatory cytokines and nitric oxide synthase by chondrocytes from patients with osteoarthritis. *Arthritis & Rheumatism*. 1998 Dec 1;41(12):2165-74.
  34. Mendes AC, Baran ET, Pereira RC, Azevedo HS, Reis RL. Encapsulation and survival of a chondrocyte cell line within xanthan gum derivative. *Macromolecular bioscience*. 2012 Mar;12(3):350-9.
  35. Mollon B, Kandel R, Chahal J, Theodoropoulos J. The clinical status of cartilage tissue regeneration in humans. *Osteoarthritis and cartilage*. 2013 Dec 1;21(12):1824-33.
  36. Mustafa A, Tomescu A, Mustafa E, Cherim M, Sîrbu R. Polyelectrolyte Complexes Based on Chitosan and Natural Polymers. *European Journal of Interdisciplinary Studies*. 2016 Apr 30;4(1):100-7.
  37. Ng MK, Weiss P, Yuan X. Solving constrained total-variation image restoration and reconstruction problems via alternating direction methods. *SIAM journal on Scientific Computing*. 2010 Aug 31;32(5):2710-36.
  38. O'Brien FJ. Biomaterials & scaffolds for tissue engineering. *Materials today*. 2011 Mar 1;14(3):88-95.

39. Ouyang L, Highley CB, Rodell CB, Sun W, Burdick JA. 3D printing of shear-thinning hyaluronic acid hydrogels with secondary cross-linking. *ACS Biomaterials Science & Engineering*. 2016 Jun 9;2(10):1743-51.
40. Paiva D, Gonçalves C, Vale I, Bastos MM, Magalhães FD. Oxidized Xanthan Gum and Chitosan as Natural Adhesives for Cork. *Polymers*. 2016 Jul 14;8(7):259.
41. Pal CP, Singh P, Chaturvedi S, Pruthi KK, Vij A. Epidemiology of knee osteoarthritis in India and related factors. *Indian journal of orthopaedics*. 2016 Sep;50(5):518.
42. Park H, Temenoff JS, Holland TA, Tabata Y, Mikos AG. Delivery of TGF- $\beta$ 1 and chondrocytes via injectable, biodegradable hydrogels for cartilage tissue engineering applications. *Biomaterials*. 2005 Dec 1;26(34):7095-103.
43. Rathke TD, Hudson SM. Review of chitin and chitosan as fiber and film formers. *Journal of Macromolecular Science, Part C: Polymer Reviews*. 1994 Aug 1;34(3):375-437.
44. Ribeiro JC, Vieira RS, Melo IM, Araújo VM, Lima V. Versatility of chitosan-based biomaterials and their use as scaffolds for tissue regeneration. *The Scientific World Journal*. 2017;2017.
45. Saito T, Takahashi T. Comprehensible rendering of 3-D shapes. In *ACM SIGGRAPH Computer Graphics 1990 Sep 1 (Vol. 24, No. 4, pp. 197-206)*. ACM.
46. Sarasam A, Madihally SV. Characterization of chitosan–polycaprolactone blends for tissue engineering applications. *Biomaterials*. 2005 Sep 1;26(27):5500-8.
47. Schmidt MB, Chen EH, Lynch SE. A review of the effects of insulin-like growth factor and platelet derived growth factor on in vivo cartilage healing and repair. *Osteoarthritis and cartilage*. 2006 May 1;14(5):403-12.
48. Sophia Fox AJ, Bedi A, Rodeo SA. The basic science of articular cartilage: structure, composition, and function. *Sports health*. 2009 Nov;1(6):461-8.
49. Suh JK, Matthew HW. Application of chitosan-based polysaccharide biomaterials in cartilage tissue engineering: a review. *Biomaterials*. 2000 Dec 15;21(24):2589-98.

50. Tan H, Chu CR, Payne KA, Marra KG. Injectable in situ forming biodegradable chitosan–hyaluronic acid based hydrogels for cartilage tissue engineering. *Biomaterials*. 2009 May 1;30(13):2499-506.
51. Tang YF, Du YM, Hu XW, Shi XW, Kennedy JF. Rheological characterisation of a novel thermosensitive chitosan/poly (vinyl alcohol) blend hydrogel. *Carbohydrate Polymers*. 2007 Feb 19;67(4):491-9.
52. Temenoff JS, Athanasiou KA, Lebaron RG, Mikos AG. Effect of poly (ethylene glycol) molecular weight on tensile and swelling properties of oligo (poly (ethylene glycol) fumarate) hydrogels for cartilage tissue engineering. *Journal of Biomedical Materials Research Part A*. 2002 Mar 5;59(3):429-37.
53. Truong-Le VL, August JT, Leong KW. Controlled gene delivery by DNA–gelatin nanospheres. *Human gene therapy*. 1998 Aug 10;9(12):1709-17.
54. Ventola CL. Medical applications for 3D printing: current and projected uses. *Pharmacy and Therapeutics*. 2014 Oct;39(10):704.
55. von der Mark K, Gauss V, von der Mark H, Müller P. Relationship between cell shape and type of collagen synthesised as chondrocytes lose their cartilage phenotype in culture. *Nature*. 1977 Jun;267(5611):531.
56. Weiss P, Fatimi A, Guicheux J, Vinatier C. Hydrogels for cartilage tissue engineering. In *Biomedical Applications of Hydrogels Handbook 2010* (pp. 247-268). Springer, New York, NY.
57. Wilusz RE, Sanchez-Adams J, Guilak F. The structure and function of the pericellular matrix of articular cartilage. *Matrix biology*. 2014 Oct 1;39:25-32.
58. Woodfield TB, Malda J, De Wijn J, Peters F, Riesle J, van Blitterswijk CA. Design of porous scaffolds for cartilage tissue engineering using a three-dimensional fiber-deposition technique. *Biomaterials*. 2004 Aug 1;25(18):4149-61.
59. You F, Wu X, Zhu N, Lei M, Eames BF, Chen X. 3D Printing of porous cell-laden hydrogel constructs for potential applications in cartilage tissue engineering. *ACS Biomaterials Science & Engineering*. 2016 Jun 30;2(7):1200-10.
60. Zhong L, Ostrom M, Truex MJ, Vermeul VR, Szecsody JE. Rheological behavior of xanthan gum solution related to shear thinning fluid delivery for

subsurface remediation. *Journal of hazardous materials*. 2013 Jan 15;244:160-70.

61. Zhu W, Wang J, Wang S, Gu Z, Aceña JL, Izawa K, Liu H, Soloshonok VA. Recent advances in the trifluoromethylation methodology and new CF<sub>3</sub>-containing drugs. *Journal of Fluorine Chemistry*. 2014 Nov 1;167:37-54.
62. Zonana J, Elder ME, Schneider LC, Orlow SJ, Moss C, Golabi M, Shapira SK, Farndon PA, Wara DW, Emmal SA, Ferguson BM. A novel X-linked disorder of immune deficiency and hypohidrotic ectodermal dysplasia is allelic to incontinentia pigmenti and due to mutations in IKK-gamma (NEMO). *The American Journal of Human Genetics*. 2000 Dec 1;67(6):1555-62.